MOTOR UNIT ESTIMATES THROUGH ACCELEROMETRY

MOTOR UNIT ESTIMATES THROUGH ACCELEROMETRY

By

DOUG ELEVELD, B.ENG.

A Thesis

for the Degree

Master of Engineering

McMaster University

September 1992

MASTER OF ENGINEERING
(Electrical Engineering)

McMASTER UNIVERSITY
Hamilton, Ontario

TITLE: MOTOR UNIT ESTIMATES THROUGH ACCELEROMETRY

AUTHOR: Doug Eleveld, B.ENG. (McMaster University)

SUPERVISOR: Dr. H. de Bruin

NUMBER OF PAGES xii, 133

ABSTRACT

Accelerometers were used to measure evoked peak limb acceleration (EPLA) for the fourth (index) finger. EPLAs were used to investigate force properties of motor units (MUs) and estimate their numbers in the first dorsal interosseous (FDI) through clustering in the force versus stimulus amplitude relationship. This system was semi-automated using a personal computer with A/D and D/A facilities. Upon repeated excitation, some MUs would potentiate and increase their force contribution by 3 to 4 times. It was found that MU number estimation procedures based on force that do not consider twitch potentiation may be underestimating MU numbers. A disadvantage of using EPLA for MU estimation is that sensitivity may vary between subjects due to finger weight and joint dynamics.

ACKNOWLEDGEMENTS

I would like to thank McMaster University and Dr. H. De bruin for making this thesis financially possible. I would also like to thank John Smerek for his help in evaluating some of my ideas and my friends and family for being supportive. A special thanks goes to my companion Helen Wong for help in editing and putting up with my numerous idiosyncrasies.

TABLE OF CONTENTS

CHAPTER 2. HARDWARE

CHAPTER 3. SOFTWARE

LIST OF ILLUSTRATIONS

LIST OF TABLES

LIST OF ABBREVIATIONS

EPLA	Evoked peak limb acceleration
EMG	Electromyography
FDI	First dorsal interosseous
MELA	Maximum evoked limb acceleration
MU	Motor unit

CHAPTER 1.

INTRODUCTION AND BACKGROUND

1.1 INTRODUCTION

The human neuromuscular system is very complex. The complete functioning of this system is not known for healthy individuals or individuals with neuromuscular disease. A better understanding of our neuromuscular system would help in the treatment, diagnosis and prevention of neuromuscular diseases. This thesis focuses on the use of accelerometers for the investigation of human neuromuscular properties.

A motor unit (MU) is the smallest unit of contraction of human skeletal muscle. Excitation of the MU produces an electrical and a mechanical response. A technique developed by McComas and his colleagues (1971) using evoked electromyography (EMG) has established single MU electrical responses and estimates of the total number of MUs in a muscle. There are several variations on this technique. (Ballantyne and Hansen, 1974; Panayiotopoulos et al., 1974; Milner-Brown and Brown, 1976; Jasechko, 1987; Cavasin 1989) However, arguments about recruitment bias (Kadrie et al., 1976), alternation (McComas et al., 1971) and nonlinear summation of EMG (Parry et al., 1977) prevent any one of those

techniques from being universally accepted.

Measurements of the evoked mechanical response of a MU, that is to say, a twitch, have been based on strain gauge instruments to measure isometric force. Measuring muscular force avoids any problems with non-linear summation of MU responses since all MUs in a muscle share common origin and insertion tendons. MU estimates have been made using twitch tension. (Burke et al., 1974; Stein et al., 1990) When measuring muscular force, the necessary force recording system must be sensitive and stable, making it difficult to construct. This is considered the most significant disadvantage of using twitch tension for MU investigation. (McComas, 1991) This thesis uses accelerometers to measure evoked peak limb acceleration (EPLA) and estimate MU numbers in skeletal muscle. It is also shown that twitch potentiation is important to consider when measuring muscle twitches.

Spike-triggered averaging (Milner-Brown et al., 1973) involves triggering a force averager from the electromyographic response of a single MU recorded with a needle electrode. The subject contracts the muscle under voluntary control. The problems of twitch fusion, recruitment bias, twitch potentiation and the invasive nature of this technique make spike-triggered averaging non-ideal.

Intramuscular microstimulation (Taylor et al., 1976) has also been used in conjunction with isometric muscular force recordings. This involves stimulating individual MUs through a needle inserted into the muscle, and measuring their force response. The stimulating electrode is necessarily close to muscle fibres, and the excitation of muscle fibres may reduce MU identification accuracy. If several twitch responses are averaged to get a MU response, then twitch potentiation can affect the responses gathered. This technique is invasive and better methods should be sought.

This thesis focuses on the use of accelerometers to measure EPLA from motor point stimulation and relates this to the force produced by the MUs of the muscle. MU numbers can be estimated by dividing the maximum evoked limb acceleration (MELA) by the average MU EPLA. The techniques described in this thesis are used to non-invasively estimate individual MU properties and the number of MUs in human first dorsal interosseous muscle (FDI). These techniques may also be applied to muscle twitches recorded on a strain gauge apparatus when the stimulus source is either motor point stimulation, intramuscular microstimulation or graded whole nerve stimulation.

1.2 SUMMARY OF CHAPTERS

Chapter 1 describes the concept of the MU and some of its properties. It also describes some of the ways in which muscular response can be measured. In Chapter 2, the hardware used in this thesis is described in detail. Software for simulation, hardware control and data analysis is described in Chapter 3. Chapter 4 examines the results of simulations and real studies on human subjects, and their respective limitations. Chapter 5 contains conclusions based on the results from Chapter 4. Finally, Chapter 6 contains some suggestions for further research.

1.3 MOTOR UNIT CONCEPT

Although a detailed description of the electrophysiological and electrochemical systems in human skeletal muscle is beyond the scope of this thesis, a brief overview follows. A more detailed description can be found in many books on electrophysiology such as Basmajian (1979).

The MU is the smallest unit of contraction in human skeletal muscle. The MU size, which is a reference to the number and strength of muscle fibres innervated by that unit, determines the magnitude of muscular contraction. Figure 1 shows an overview of the MU morphology. The motor neuron cell

Figure 1: Motor Unit Morphology

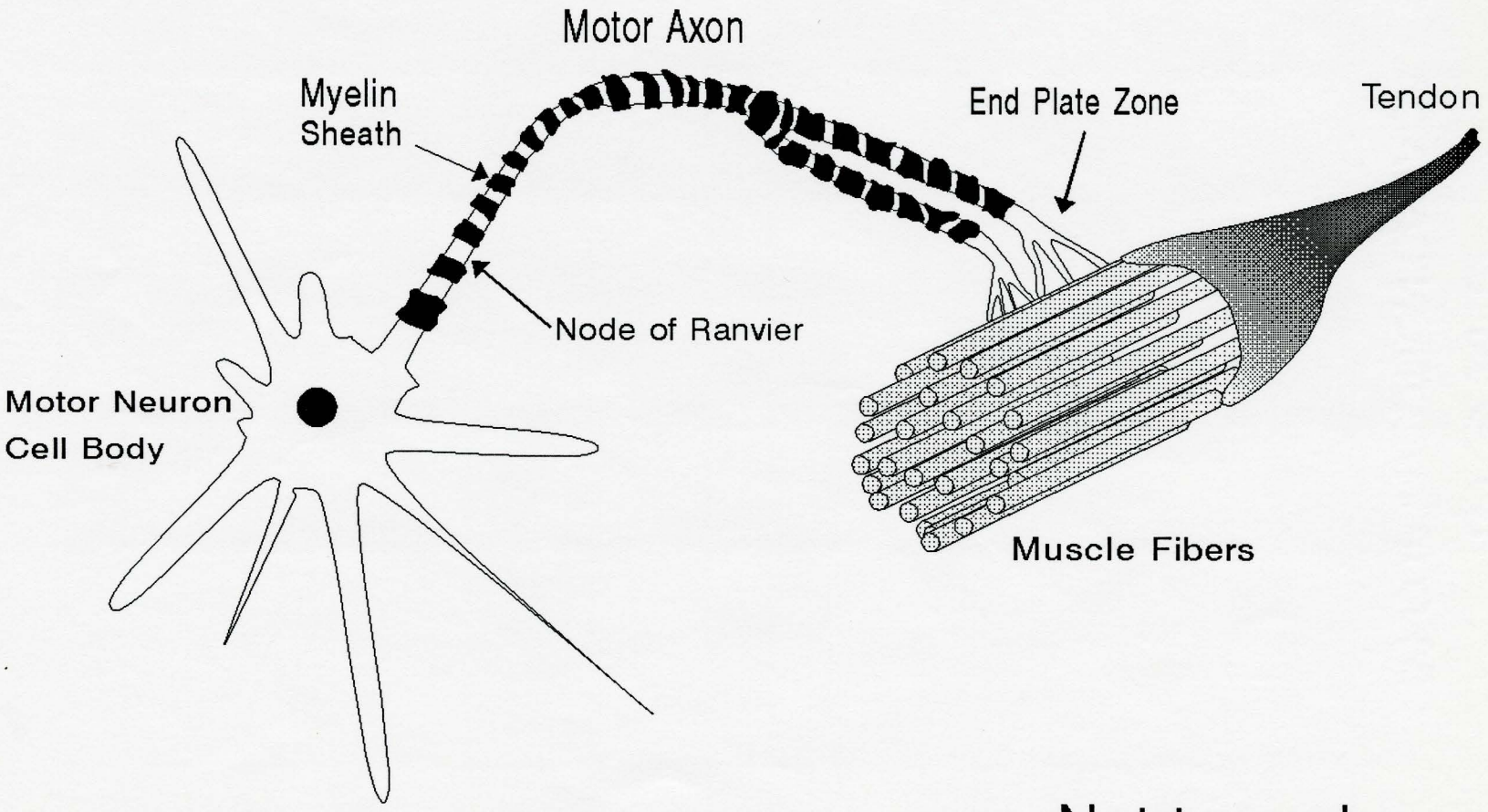

Not to scale

body is located in the spinal column, and a motor axon branches off the cell body. The motor axon is protected by a myelin sheath which also has the effect of greatly increasing the velocity of electrical transmission along the axon. The axon branches into dendrites which in turn innervate muscle fibres. A single MU may innervate a range of a few to several hundred muscle fibres depending on the muscle. The number of MUs in a muscle varies over the same range.

Excitation of the motor neuron causes contraction of all the muscle fibres that are innervated by the neuron. The excitation of the motor neuron and subsequent contraction of the muscle fibres is an all-or-nothing event. Either the MU fully contracts and produces a twitch, or it does not contract. For normal, healthy MUs there are no partial MU contractions. Motor neuron excitation occurs in the form of a rapid depolarization and then repolarization of the cellular membrane. A zone of depolarization travels along the motor neuron across synaptic gaps at the terminal branches and initiates complex chemical, electrical and mechanical responses in the associated muscle fibres.

The motor axon is demyelineated just before it enters the muscle. This area is called the end plate zone. If a current is passed through this area, some or all of the MUs of the

muscle will be excited depending on the intensity and spatial distribution of the current and the thresholds of the MUs.

The force produced by the muscle fibres pulls on the connective tissue of the muscle, transmitting force to the muscle tendons. The tendons in turn transmit force to their associated origins and insertions. Since all MUs in a muscle transmit force through common tendons, the force addition of 2 or more MU is linear. If at least one of the tendons is attached to a limb that is free to move, the excitation of the motor neuron will cause the muscle to shorten causing movement of the limb.

If the MU is stimulated and the associated limb is free to move, then the limb will twitch. The force of the MU contraction causes the limb to accelerate. After about 150 milliseconds, the force production of the MU has ceased and the limb returns to its resting position. The magnitude of limb movement depends on muscular contraction force, limb dynamics and joint properties.

MU numbers can be estimated by dividing the MELA by the average MU EPLA contribution. The average MU EPLA contribution can be estimated by averaging the EPLAs of several MUs.

1.4 GRADED STIMULATION

If an electric current is passed through the area of the end plate zone, a motor axon may become stimulated, resulting in a muscular contraction. The muscle can then be studied as an input-output system in which the input can be controlled. Of course, the subject should not be providing electrical signals to the muscle during the study period. This can be achieved by having the subject relax the muscle involved.

The stimulation of a MU depends on the physical geometry of the motor axon and the electrodes, the MU electrical thresholds and the stimulus amplitude. Since the physical geometry of the motor axon cannot be changed without resorting to destructive or invasive techniques, control over the stimulation must be achieved with careful electrode placement and by varying stimulus amplitude.

The voltage at the motor neuron must be higher than the threshold before it will be excited and produce a twitch. So, passing an extremely small electrical current through the end plate zone will not excite any motor axons. Conversely, if a very large current is passed through the end plate zone, then all of the motor axons will be excited. It follows that fine control over stimulus amplitude is necessary for a subset of the motor axons that pass through the end plate zone to be

stimulated. The computer controlled stimulator used in this thesis had a minimum step size in stimulus voltage of 24.4 mV. This fine control is adequate for excitation of MU subsets. A complete description of the stimulator hardware can be found in Chapter 2. Also, a complete description of stimulating electrode setup can be found in Section 2.4.2.

1.5 ALTERNATION

A MU will only fire if the stimulus voltage (or current) is higher than the threshold for that unit. However, the exact electrical thresholds of human skeletal muscular MUs vary over time. It is therefore more convenient to speak of a range of stimuli over which the probability that a MU will fire varies from 0 to 1. Although the precise shape of this curve is not known, it is generally assumed to be a 'S' shape as shown for each MU in Figure 2.

Alternation was first described by McComas et al. (1971) and can be characterized as a variation from the most probable recruitment order. Some combinations are less likely than others. Table 1 explains in detail the possible firing patterns of the MU shown in Figure 2. At a stimulus intensity of 30 volts, MU #1 has a firing probability of 90%, MU #2 has a firing probability of 60%, and MU #3 has a firing

Figure 2

Activation Curves for Three Motor Units

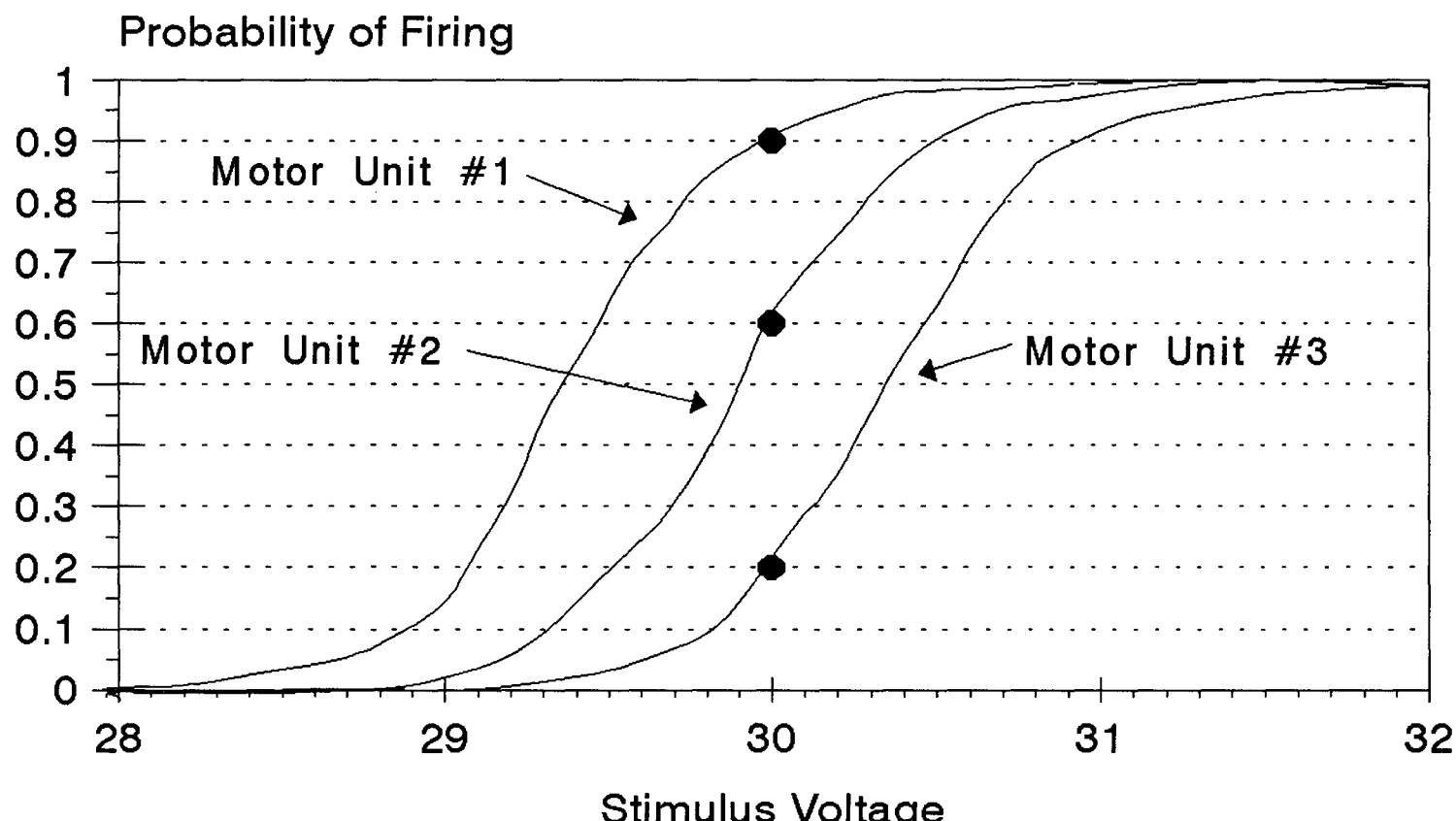

Table 1

Firing Probabilities for Three Motor Units

MUs Fired	Alternation	Probability
None	No	.1*.4*.8 = 0.032
only 1	No	.9*.4*.8 = 0.288
only 2	Yes	.1*.6*.8 = 0.048
1 and 2	No	.9*.6*.8 = 0.432
only 3	Yes	.1*.4*.2 = 0.008
1 and 3	Yes	.9*.4*.2 = 0.072
2 and 3	Yes	.1*.6*.2 = 0.012
1 and 2 and 3	No	.9*.6*.2 = 0.108

For activation curves see Figure 2

probability of 20%. Thus, at a stimulus intensity of 30 volts, there are several possible MU firing patterns.

If there are N MUs with a reasonable probability of firing, then there are 2^N different combinations possible, and $2^N-(N+1)$ of those responses will be alternated responses.

Alternation poses a problem for the MU identification process because the difference between two different evoked responses is not necessarily a discrete MU. Table 1 clearly illustrates this point. Better MU identification such as those developed by Jasechko (1987) and Cavasin (1989) try to account for simple alternation, although they are incapable of dealing with more complex alternation. A recent MU identification process briefly described by Daube (1988) avoids the problem of alternation by using Poisson analysis to determine the size of the average MU. Although wide ranges of MU sizes may cause poor results from this technique (McComas, 1991) it appears very promising.

The processes in this thesis deal with alternation by choosing data types and data sets where there is little alternation, or where alternation does not affect the MU estimation results. The explanation of this approach is complex and is described in detail in Chapter 4.

1.6 MUSCLE STUDIED

The muscle investigated in this thesis was the FDI. The placement of this muscle can be found in Figure 3. The muscle originates along the side of the metacarpal and inserts on the proximal phalanx of the index finger.

The FDI's action causes abduction and flexion of the index finger. (Tortora and Anagnostakos, 1990) This muscle's end plate zone is in the middle of the muscle just beneath the skin. It is easy to stimulate the FDI motor point using surface electrodes.

There were two primary reasons for choosing the FDI muscle for this thesis. First, detailed morphological studies of the FDI have been made. In a study by Feinstein (1955), it was assumed that 40% of the large diameter fibres are afferent. This assumption may not hold true in all persons and therefore the estimates must be interpreted with great caution. With this assumption, Feinstein et al. estimated that the FDI of a normal female consists of 119 MUs. The second reason for choosing the FDI was that it can be made to act in one dimension. If the index finger is made rigid by taping stiff steel wire to the underside and the thumb is secured, the FDI acts solely for index finger abduction. Thus its force production can be measured with a one dimensional

Figure 3: Muscle Studied

First Dorsal Interosseus

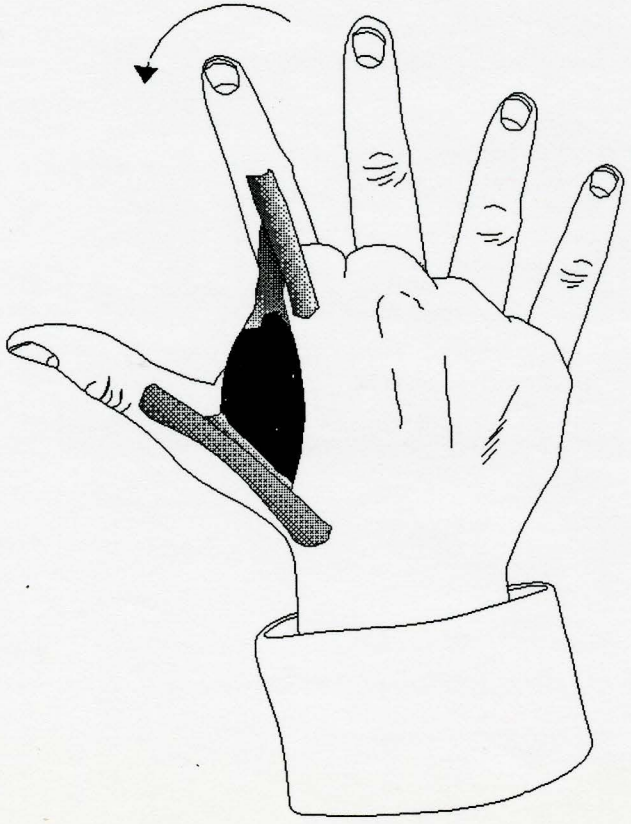

- Can be made to act in one dimension
- Easy to stimulate
- Existing morphological data

accelerometer. Furthermore, the cost of accelerometers is linearly related to the number of dimensions to be analyzed. Two dimensional accelerometers cost approximately twice as much as one dimensional accelerometers. Therefore the FDI is a good muscle to study because the accelerometer required is more economical than one required to record the action of a muscle that acts in two dimensions such as the thenar muscle.

There is also an advantage in studying a muscle such as the FDI which can be made to act in one dimension. During large stimulations it is possible that other muscles near the FDI become stimulated. A one dimensional accelerometer with its sensitive axis parallel with the action of the FDI will reject the acceleration produced by other muscles as long as those muscles do not act in the same axis as the FDI. With macro EMG, all muscles stimulated either intentionally or unintentionally will contribute to the EMG recorded regardless of the direction of their force actions. In this way, recording the action of the FDI with a one dimension accelerometer will reduce the interaction of other muscles.

1.7 RELATIONSHIP OF FORCE AND ACCELERATION

When the FDI is stimulated the index finger will accelerate laterally and twitch if it is free to move. The

mass of the index finger and the damping at the joint will interact with the force that the FDI produces and result in a movement of the index finger. Figure 4 shows the acceleration, velocity and position graphs of the index finger during a twitch. This information was obtained using the hardware described in Chapter 2. The traces have been scaled and the units removed for clarity.

The free movement of the index finger cause the response to be non-isometric, and results gathered in this manner cannot be directly compared to isometric responses. The time to peak acceleration for a free to move index finger upon stimulation of the FDI is shorter than the time to peak isometric force. This is because the FDI is shortening as peak force is produced. A study by Gravel et al. (1987) showed that when human plantarflexor muscles are stimulated during passive shortening, contraction time decreases and relaxation time increases. The peak force production during passive shortening was decreased but was just as stable and repeatable as peak force during static conditions or passive lengthening. The fact that the FDI is shortening does not affect the proportionality of the EPLA to the peak muscular force produced. Tendon elasticity was considered to be negligible at the force levels considered.

Figure 4

Index Finger Lateral Twitch

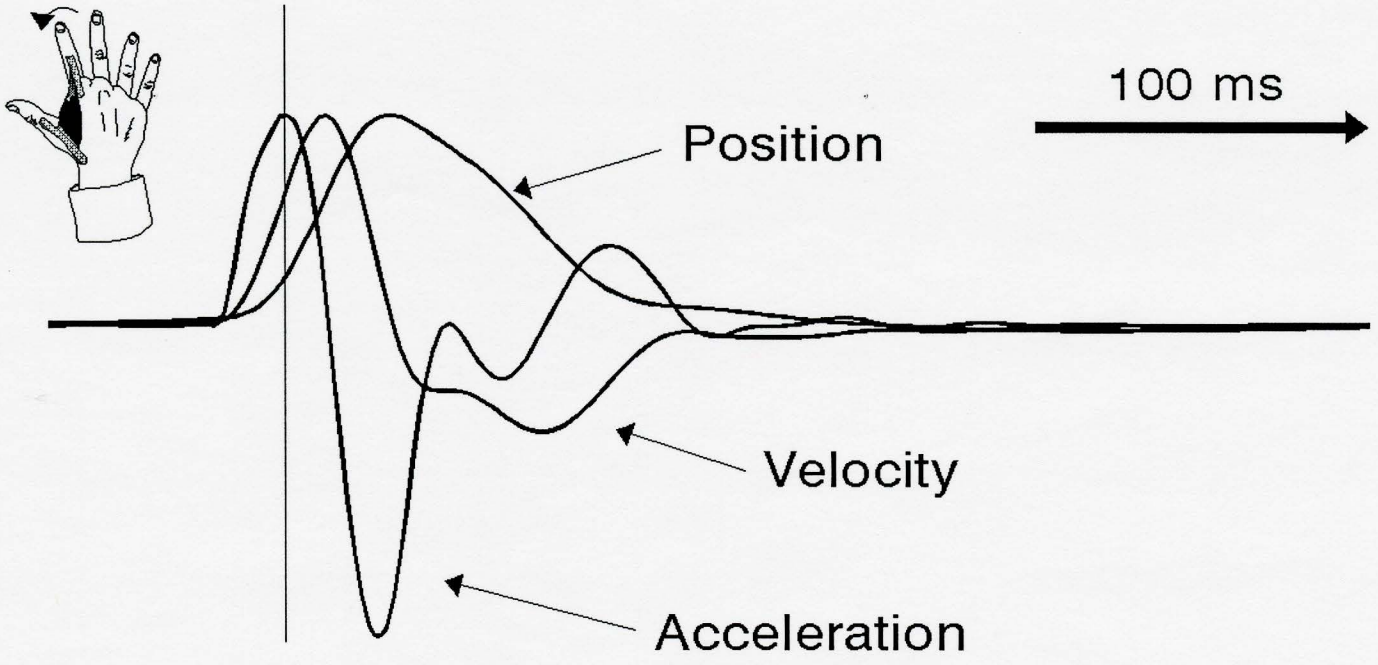

From stimulation of FDI on free-to-move index finger

The EPLA is related to the peak muscle force through the mass and damping of the index finger. The units of force cannot be accurately described unless accurate measurements of effective index finger mass and damping are calculated. It was felt that such calculations were impractical and so the EPLA must only be considered to be proportional to peak muscular force.

EPLA occurs at approximately 25 milliseconds from stimulation and the response lasts about 150 milliseconds. Isometric measurements of twitch force of FDI using strain gauges found that peak force is produced within 33 to 147 milliseconds (Stephens et al. 1977).

The magnitude of typical FDI MU EPLA contributions is approximately 5.23e-5 m/s^2. This value is derived in Section 4.3.8.

1.8 STRAIN GAUGE TECHNOLOGY

Isometric muscular force can be measured using strain gauges. Typically, the strain gauges are bonded to a metal bar and deflection of the bar is measured. Great sensitivity with adequate signal to noise ratios can be achieved through amplification of the strain gauge signals because strain

gauges typically have low resistance. However, stability of the force measurement is difficult to achieve. Respiration and blood pressure signals can affect the force measured and corrupt the isometric twitch recordings of thenar muscles. (Westling et al., 1990) This is especially important for small twitches which may become completely unrecognizable. Also, synchronization of stimulus to blood pressure and respiration significantly complicates stimulus control. Small shifts in subject position will affect the baseline force on the strain gauge, which may cause amplifier saturation if the gain is high.

Measuring limb acceleration avoids the problem of baseline shifts due the inherent self-levelling nature of the accelerometer. If the subject shifts position slightly, the accelerometer will indicate this shift, but then return to zero when the subject stops moving.

1.9 ELECTROMYOGRAPHY

Many techniques for MU investigation use macro EMG. Macro EMG is the electrical response of the firing of the nerves and muscle fibres at the surface of a muscle. Since the response is only recorded at the surface of the muscle, the depth of the MU and the actual physical extent of the MU

cannot be known. For example, a small EMG response may indicate a small MU very near the electrodes or a large MU deep in the muscle. The volume conduction of the EMG through the muscle may also be affected by non-linearities of electrical transmission through activated or non-activated muscle fibres. (Parry et al., 1977)

Furthermore, there is the problem of latency shifting. (Cavasin et al., 1989) When a MU is fired several times, its timing with respect to the stimulus may change within a few milliseconds. The macro EMG of the firing of several MUs may have a range of shapes depending on the latencies of each of the MUs. Recognizing these shapes by human operator or by computer becomes an extremely complicated task when several MUs are being stimulated at the same time. If alternation also occurs the task may become insurmountable, and alternated responses with different latencies may be interpreted as separate MUs. This would cause MU number estimates to be too high.

CHAPTER 2.

HARDWARE

2.1 BRIEF OVERVIEW

The hardware of this thesis consisted of four major parts. An accelerometer, an amplifier, a stimulator and a personal computer with D/A and A/D facilities were used. The interconnections between these component parts are shown in Figure 5.

The accelerometer, an Entran EGAX-5, was taped on the finger with its most sensitive axis in line with the abduction axis of the FDI. Stiff aluminium wire was taped to the bottom of the finger to minimize lateral finger flexibility and FDI contribution to index finger flexion.

The amplifier was a band pass, cutting off at 0.0015 Hz and at 48 Hz. DC measurement was not used because the accelerometer requires up to 4 hours of warmup time for accurate measurements at DC. (Entran International, 1987) The amplifier had 10 selectable gains from 59.7 to 28573.

The computer was a 10 Mhz 80286 AST machine with a Data

Figure 5

Hardware Overview

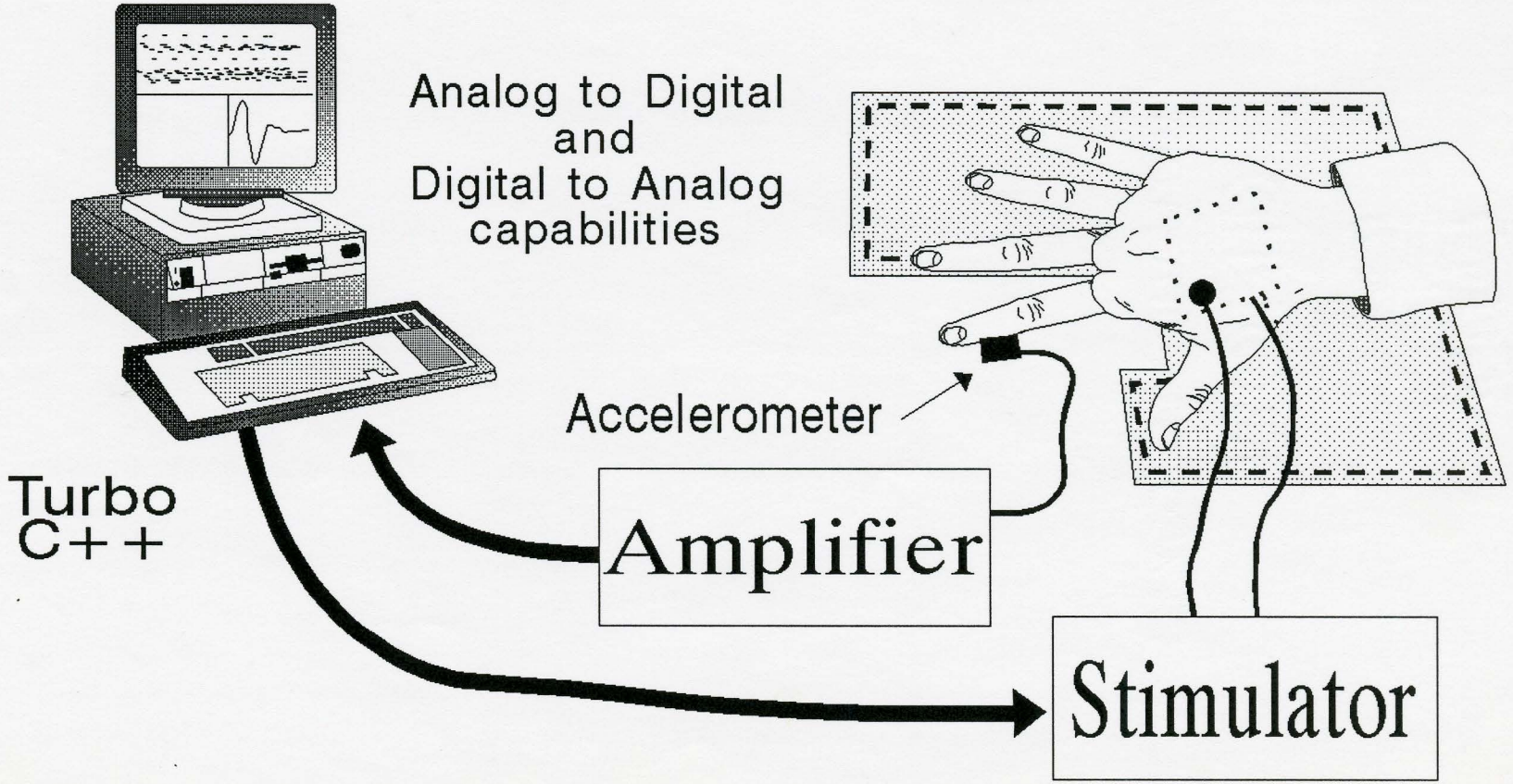

Translation DT-2801-A board. The computer read the evoked twitches through an A/D channel sampled at 4 Khz and applied several signal processing strategies to the twitches. The data were then saved to hard disk. The computer stimulated the subject's FDI and only re-stimulated when the response had sufficiently diminished. The acceleration signal was considered diminished when a pre-determined number of samples read from the A/D board were within a multiple of the standard deviation of the inherent noise of the system. In this way, the muscle could be successively stimulated as fast as possible while avoiding twitch fusion and large noise signals. The computer automatically collected a chosen number of evoked responses and saved them.

The subject's hand was placed in a restraining device to minimize the interference of subject movement to the acceleration measurements. The restraining device also provided some mechanical decoupling from mechanical noise sources such as computer fans and air conditioning equipment.

2.2.1 ACCELERATION TRANSDUCER

The accelerometer chosen for this study was an Entran EGAX-5. It has a range of +/-5g (1g = 9.8 m/s^2) and an overrange of +/-10000 g. It is compensated for accurate

operation from 70°F to 170°F, and can operate within -40°F to 250°F. The sensitivity is approximately 10 mV/g with a 15 volt excitation.

The device weighs approximately 0.5 grams without its leads. The light weight of this unit allowed maximum sensitivity. If the accelerometer was a heavy one, the mass that had to be accelerated by the muscle would have increased, thus the acceleration produced per unit of force would have decreased. A light accelerometer means that the accelerometer does not significantly affect the force causing the acceleration.

The frequency response of the accelerometer is from DC to a 3 dB point at 500 Hz. Since the amplifier has a passband from 0.0015 Hz to 48 Hz, the frequency response of the accelerometer was more than what was required.

Complete specifications for the accelerometer used can be found in Appendix 1.

The accelerometer is a fairly common unit except for its overrange capabilities. The extremely high overrange makes the accelerometer rugged and reliable. Accelerometers with lower overranges are easily destroyed by normal handling

procedures and many can be destroyed by simply clipping the leads with standard diagonal-nose pliers. Although the Entran EGAX-5 is significantly more expensive than accelerometers with lower overranges, its extreme ruggedness allows it to outlast the cheaper units.

2.2.2 ACCELEROMETER MOUNTING

The accelerometer mounting can be seen in Figure 6.

The stiff wire taped to the bottom of the finger eliminated the FDI contribution to finger flexion. The wire may also act to reduce the elastic component in the finger, causing the accelerometer to follow the force production of the muscle more closely. The accelerometer was then placed on the distal phalanx of the fourth (index) finger, thereby increasing the lever arm through which acceleration is measured. This placement was also found to increase the sensitivity of the acceleration measurement on some subjects.

The accelerometer could also be attached at the distal end of the proximal phalanx of the fourth (index) finger. However, the sensitivity may be reduced because the accelerometer would be on a shorter lever from the muscle and some FDI force may then contribute to index finger flexion.

Figure 6

Two Accelerometer Mounting Methods

Method 1

Mounted on distal phalanx of fourth finger

Method 2

Mounted distal end of proximal phalanx of fourth finger

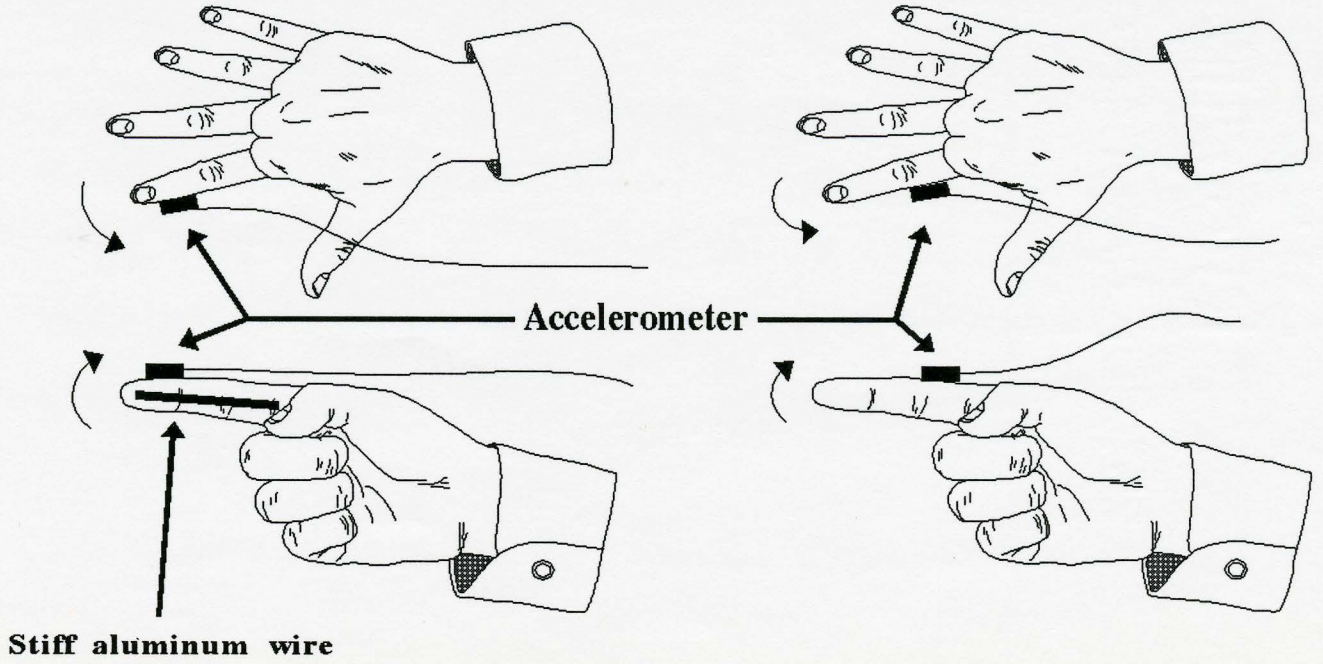

This placement would not require the use of the stiff wire, thereby reducing the mass to be accelerated.

Since each person has a unique joint structure, the mounting method used should be one that provides the greatest sensitivity.

2.2.3 ACCELEROMETER FREQUENCY RESPONSE

Figure 7 and Figure 8 show an isometric force time response of an FDI and its frequency response recorded using a strain gauge. The force production of human muscle does not appear to have significant information above 30 Hz.

Figure 9 and Figure 10 show an acceleration time response and its frequency response respectively. The shape of the time response is determined by the force production filtered by the mechanical properties of the finger and joint.

The accelerometer is limited in frequency to about 500 Hz. Since the upper frequency of recorded human muscle acceleration twitches is about 50 Hz as shown in Figure 10, the accelerometer has plenty of bandwidth. Additional filtering was done in the amplifier and will be described in the following section.

Figure 7

Isometric FDI Twitch
Time response

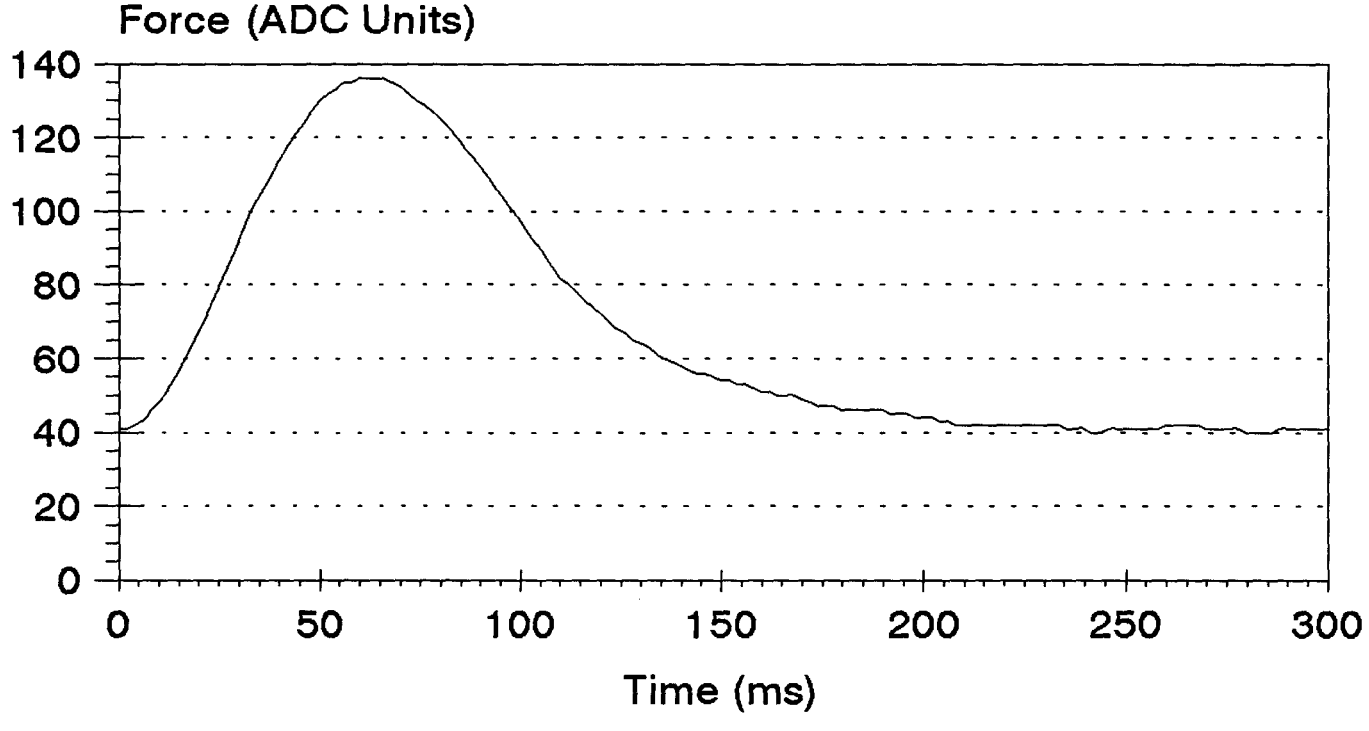

Figure 8

Isometric FDI Twitch Frequency Response

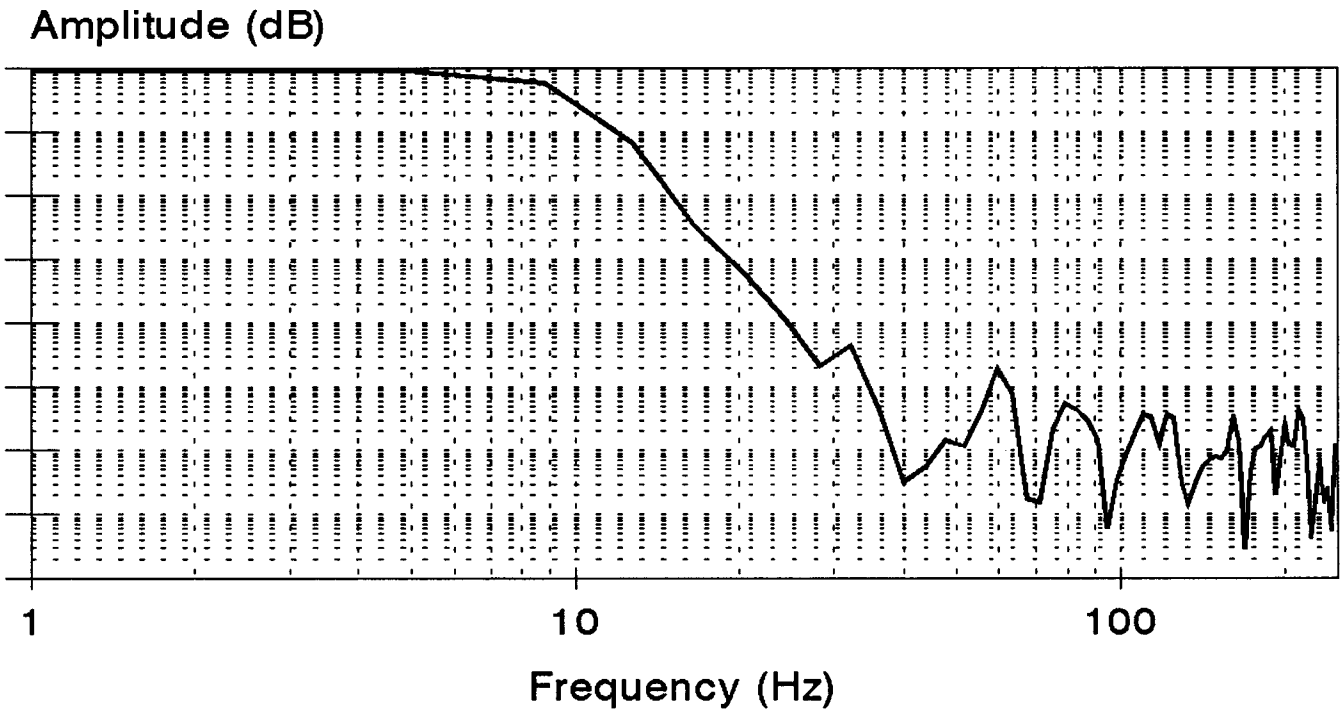

Figure 9

Acceleration FDI Twitch
Time response

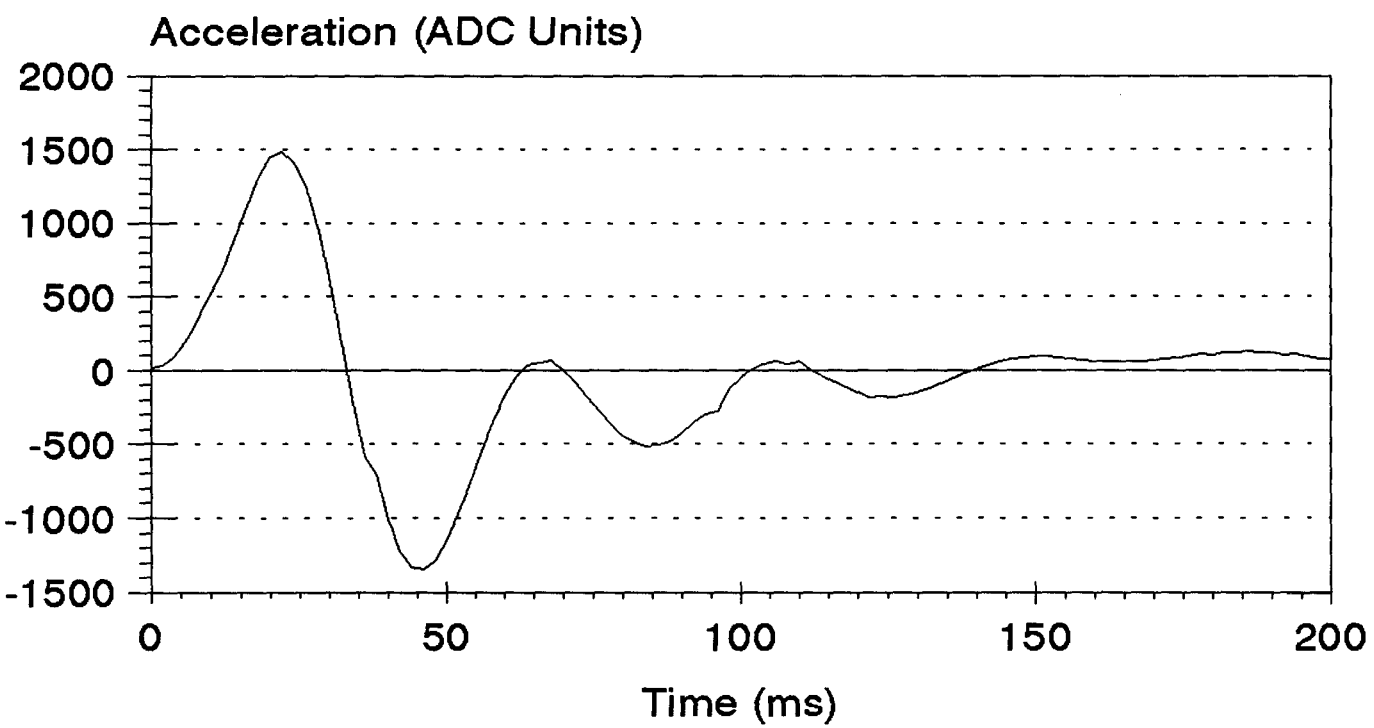

Figure 10

Acceleration FDI Twitch Frequency Response

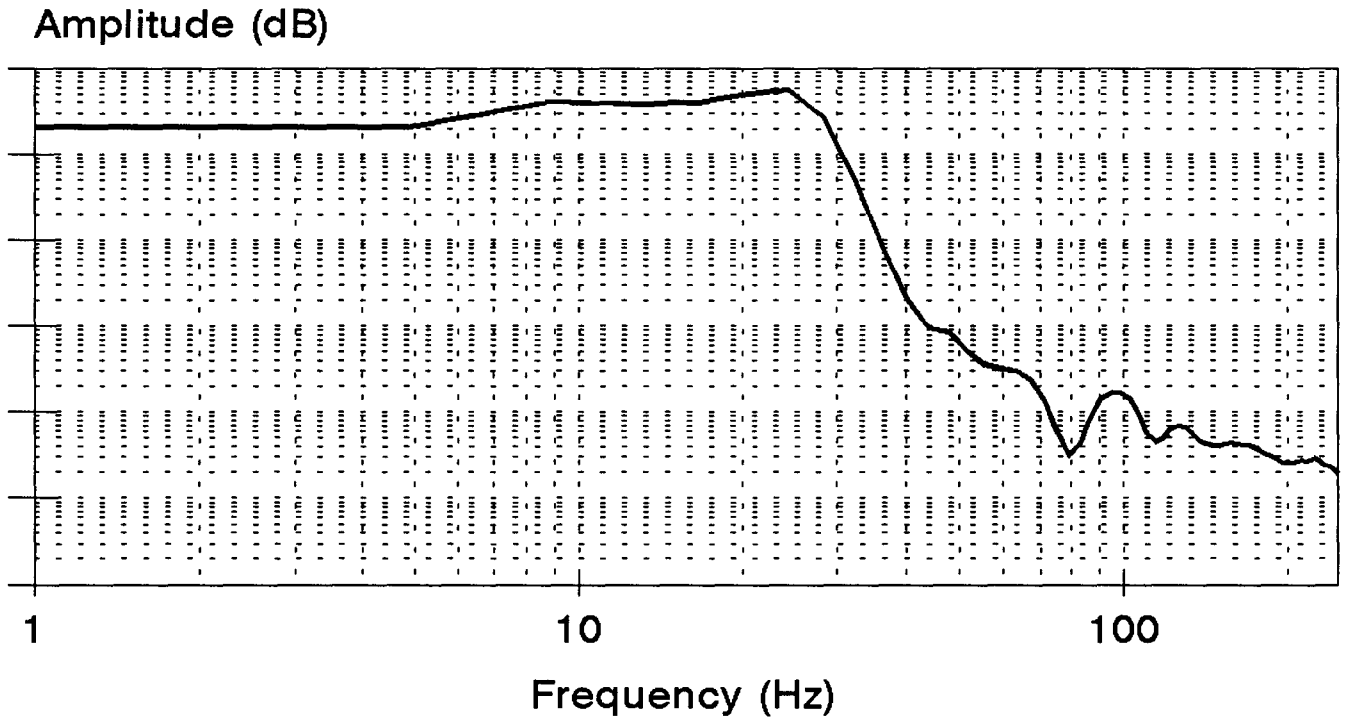

2.2.4 ACCELERATION AMPLIFIER DESIGN

The schematic diagram of the acceleration amplifier is shown in Figure 11. It was based on a circuit shown in the 1990 Linear Technology data sheet for the LT1007 opamp (Linear Technology, 1990). A brief explanation of its operation follows.

Zener diode, ZD1, maintains a 7 volt reference for the excitation voltage of the accelerometer. The R1 and C1 combination provide decoupling and reduce the noise in the excitation voltage. U2 is connected as a buffer amplifier and provides the necessary current for a 7 volt excitation at one of the excitation leads of the accelerometer. U3 holds one of the output leads of the accelerometer at 0 volts. This is achieved by the output of U3 varying the negative excitation voltage. The signal at the output of U3 would be half of the differential signal from the accelerometer minus the common mode signal minus the excitation voltage. The input of U4 which is the other output lead of the accelerometer contains half of the accelerometer differential signal plus the common mode signal plus half of the voltage seen at the output of U3. The common mode signals cancel and the differential signals add at the input of U4. The input to U4 is therefore the full differential signal with no common mode signal. The common mode signals will completely cancel if the opamps are perfect

Figure 11

Accelerometer Amplifier Schematic Diagram

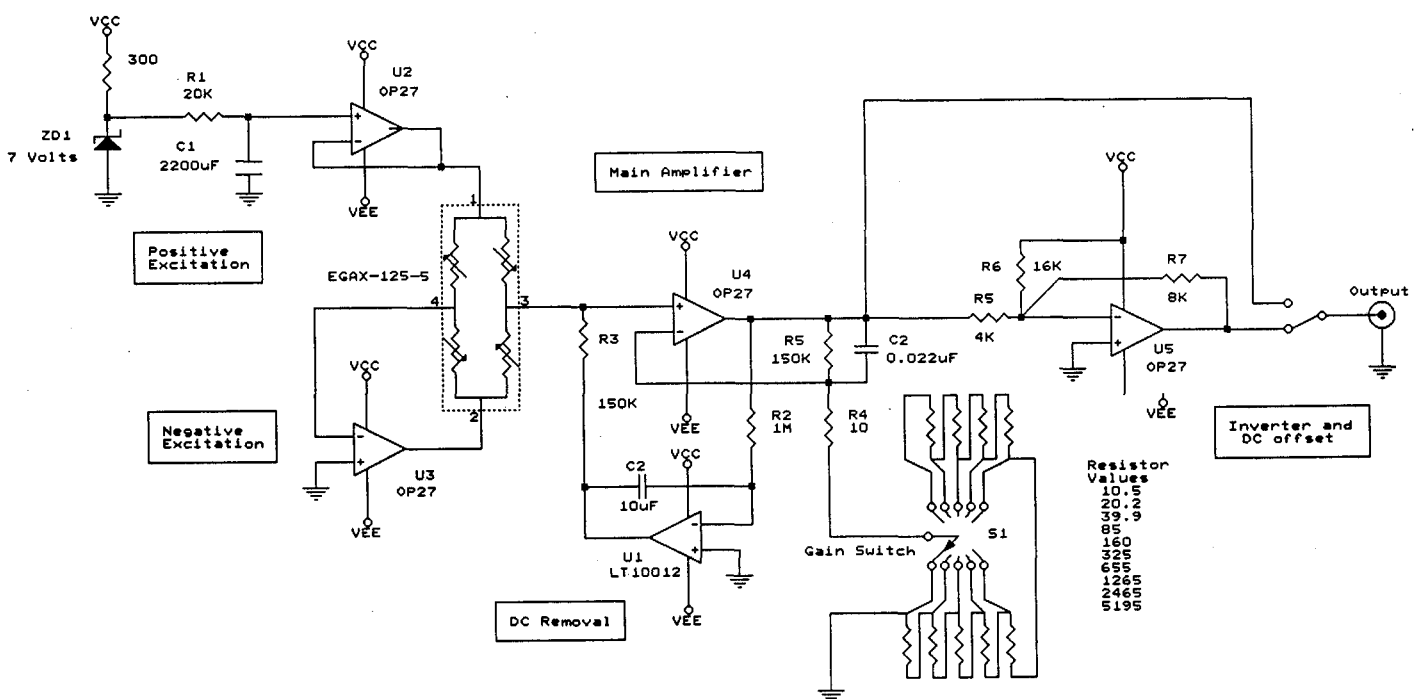

and will partially cancel in reality.

U1 samples the output voltage through R2 and provides a correction current through R3 to the input of U4. This amplifier is configured as an integrator. It effectively filters frequencies lower than those defined by the R2-C2 combination out of the output, holding the output quiescent value very close to zero volts. U5 is configured as a non-inverting amplifier with its gain defined by R5 and the series combination of R4 and the switched resistor network. The R5-C2 combination defines a first order 48 Hz low pass filter for the acceleration signal, thereby reducing the noise at the output.

U5 provides a gain of 2 and a DC offset of approximately -7.5 volts. Positive peak acceleration was the primary interest and an offset of -7.5 volts allowed greater gain before the +-10 volt limit of the analog to digital conversion was reached. Thus greater resolution of the positive peak acceleration was achieved.

2.3.1 NOISE SOURCES

There were five major contributors to the noise signal of the accelerometer. They consisted of blood pressure, air

movements, mechanical signals transmitted through the mounting, electronic noise sources and sources due to nervous action of muscles in the subject.

2.3.2 BLOOD PRESSURE NOISE

Blood pressure contributes to the noise signal of the accelerometer by acting as a variable pressure and the arteries in the finger may act as a Bourdon tube causing movement of the finger. Also, blood vessels between the accelerometer and the nearest index finger bone may vary in volume due to changes in blood pressure with each heartbeat. To evaluate the significance of these types of noise, the subject's hand was placed on the mounts and an accelerometer was attached using mounting option 1 as shown in Figure 6. The noise waveform was observed on an oscilloscope and a cuff was then inflated over the upper arm, cutting off blood flow below the cuff. The cuff ensured that no changes in blood pressure of the lower arm occurred and the reduction of the amplitude of the noise signal upon cuff inflation indicates the contribution of blood pressure to the noise signal. Figure 12 shows typical noise traces with and without an inflated cuff. When the cuff was inflated, no significant drop of the amplitude or change in the characteristics of the noise signal was noted. Therefore the contribution of blood pressure to the noise signal was considered to be minimal.

Figure 12

Blood Pressure Noise Evaluation

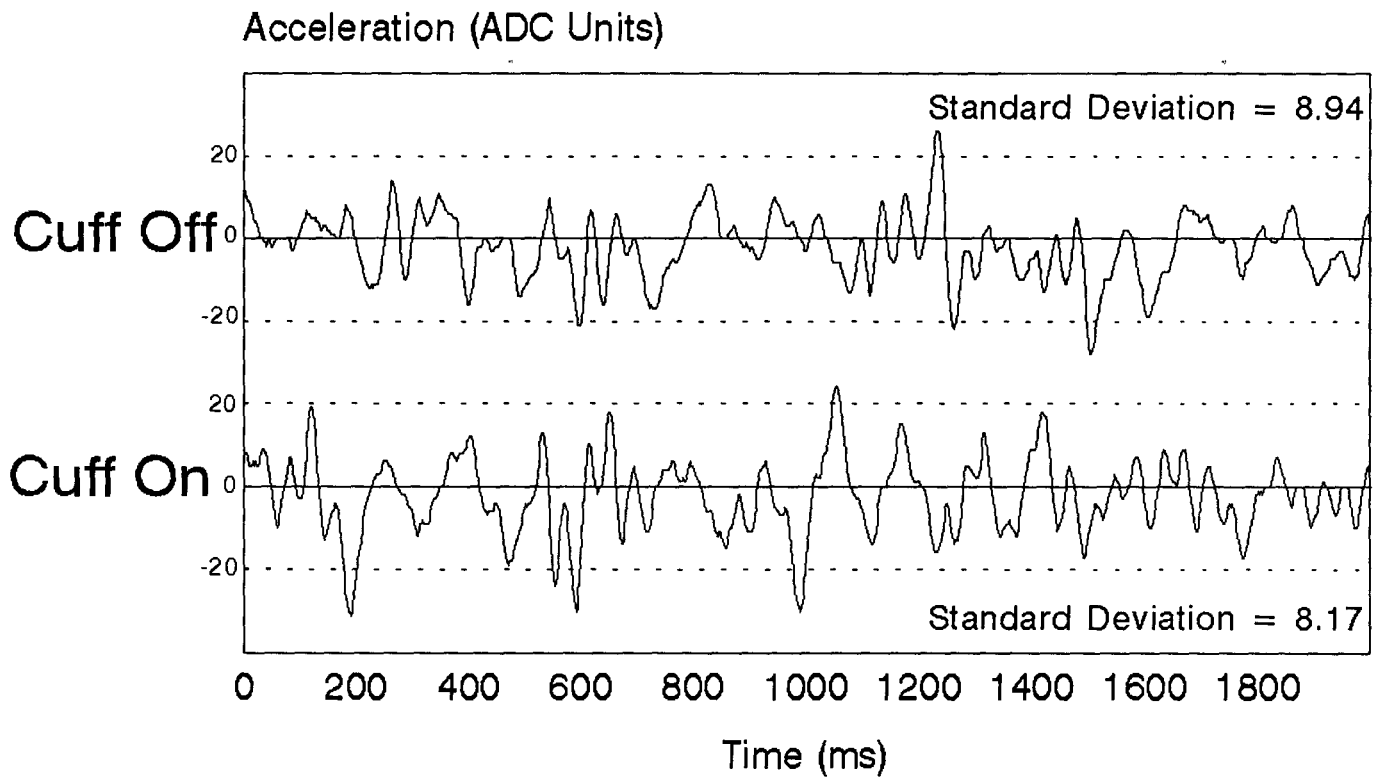

Blood pressure and respiration significantly affects the MU measurements as in thenar muscle force studies using strain gauges (Westling et al., 1990), but they do not when accelerometers are used. This was probably due to the high pass filtering in the accelerometer amplifier, the inherent self-levelling nature of accelerometers and the lack of significant changes in volume of blood vessels between the accelerometer and the nearest index finger bone.

2.3.3 AIR MOVEMENT NOISE

Air movements were a significant noise contributor and easily affected the 0.5 gram accelerometer when it was not mounted on a finger. When the accelerometer was mounted to a subject's finger, the weight to be moved by air currents was greatly increased, thus greatly decreasing the contribution of air movements to the noise signal. Since placing an air-current shield around the finger with the accelerometer attached did not significantly reduce the amplitude of the noise signal, the contribution of air currents to the noise signal was considered to be minimal.

2.3.4 MECHANICAL SOURCE NOISE

There were many sources of mechanical noise in the accelerometer noise signal. Fans, motors, and other equipment with moving parts (including humans!) around the subject caused vibrations that were transmitted to the accelerometer through the building, table, and mountings. The effect of these sources on the accelerometer noise signal was reduced by decoupling the mounting plate from the support on which the mounting rests. This was done by making the mounting plate and the cover plate out of very thick heavy pieces of metal and placing a compliant material between the mounting plate and its support (usually a table). The compliant material and the heavy mounting plate provided mechanical decoupling between the mounting plates and the support surface.

The effectiveness of the decoupling between the support surface was evaluated in the following manner. The mounting plate acceleration recordings were made with a subject's hand in the mounting plate and compared with the same subject's hand resting on the table beside the mounting plate. In each case the subject was instructed to relax their hand muscles as much as possible. Figure 13 show these two data sets. The noise recordings with the subject's hand on the mounting plate had a lower standard deviation than the recordings with the subject's hand on the table. Therefore, the mounting plate

Figure 13

Mechanical Noise Sources

In Base

On Table

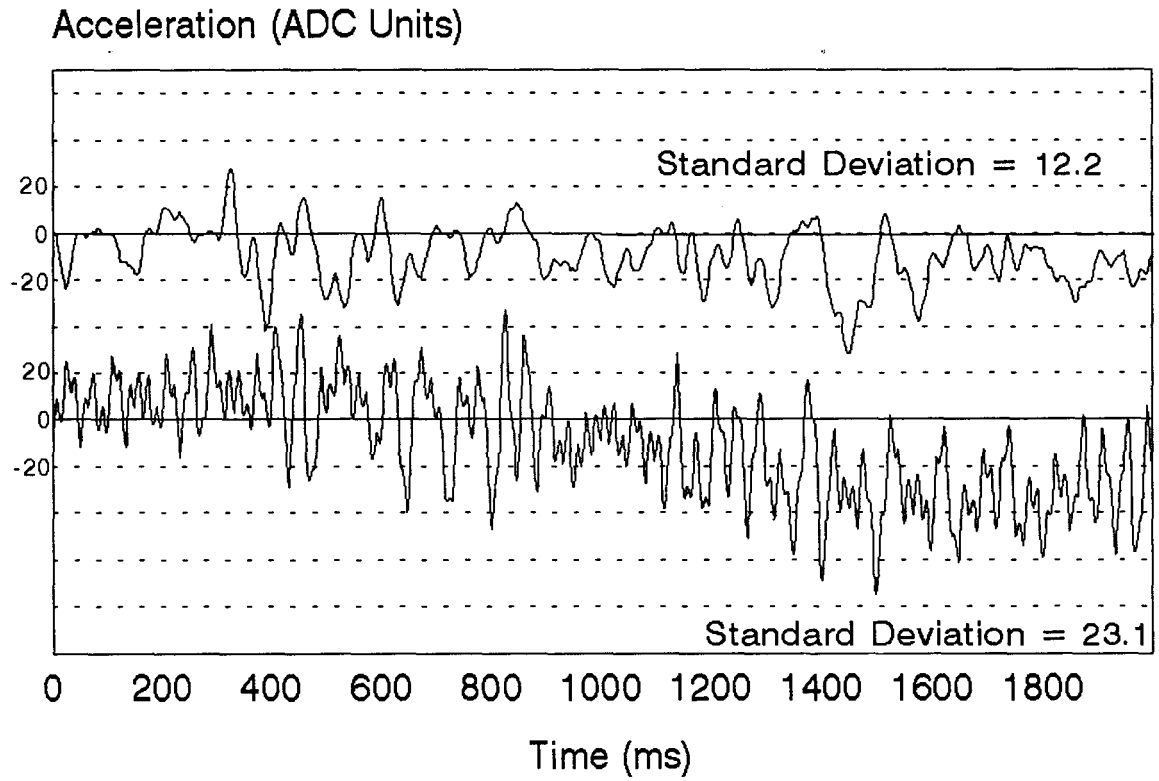

reduced the total noise contributed by mechanical sources by decoupling the mechanical vibration from the surface on which the subjects hand rested. Higher order electronic filters or digital filtering in software may further reduce the mechanical noise in the acceleration signal, however they were not employed in this thesis.

2.3.5 ELECTRONIC NOISE

The contribution of electronic sources to noise in the accelerometer noise signal was evaluated by using a dummy input load for the accelerometer. This dummy input load is shown in Figure 14 and has similar input and output impedances to the accelerometer. Figure 15 shows a typical time response of the digitally converted output of the accelerometer amplifier with the dummy input load and a gain setting of 14287. This time response contains the noise response of the amplifier circuit plus the effects of 60 Hz fields around the amplifier. The digital conversion parameters are discussed in Section 2.5.1. The standard deviation of the recording shown in Figure 15 was less than 1 ADC unit. With the accelerometer mounted on a subjects hand, the standard deviation of a noise trace are typically around 12 ADC units for the same gain. (See Section 2.3.4) Therefore, the electronic noise sources for this amplifier were not a significant contributor to acceleration noise.

Figure 14
Dummy Accelerometer

Accelerometer
EGAX-5

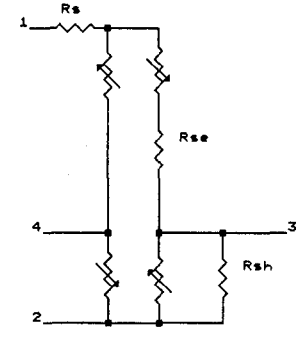

Input Impedance = 811 ohms
Output Impedance = 458 ohms

Accelerometer
Dummy Input Load

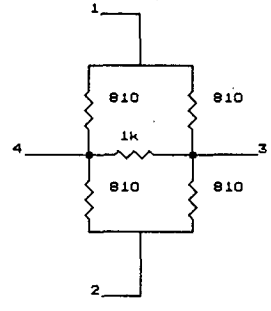

0

Figure 15

Electronic Noise Evaluation
Time response

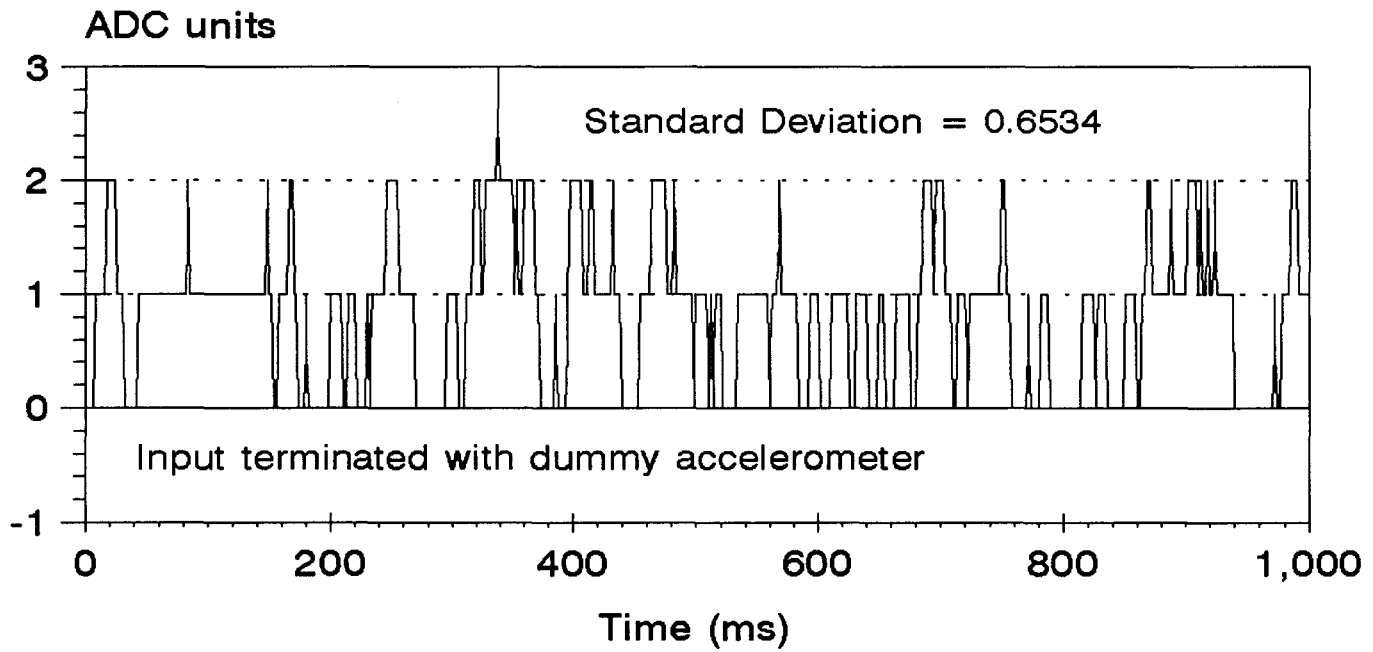

Gain setting = 14287

2.3.6 MUSCLE CONTROL NOISE

Finally, the involuntary actions of muscles were also sources of noise. Activity in other muscles around the FDI caused the index finger to vibrate. The only way to stop this noise at the source was to give the subject a muscle relaxant. The application of drugs was not considered practical for this thesis because of safety and legal concerns.

Involuntary control noise could not be experimentally separated from noise caused by external mechanical sources. Both noise sources were filtered by the dynamics of the index finger and therefore could not be filtered from the acceleration twitch response. Neither noise sources could be easily stopped at their origins. Also, inadvertent stimulation of muscles other than the FDI due to poor electrode placement may also have contributed to errors in the acceleration measurement. However the contribution of other muscles to EPLA is dependent on the alignment of the action of the other muscles with the FDI. This is explained in greater detail in Section 1.6.

Subject concentration and relaxation were the only methods used to lower the contribution of involuntary control sources of noise to the MU contribution to acceleration measurement error.

2.4.1 STIMULATOR TYPE

The stimulator used in this project was a constant voltage stimulator, Digitimer Stimulator type 3072. It was originally modified for computer control by Jasechko (1987) for his work on automatic MU estimation. Some small changes were made to his modification for stimulator control through the DT-2801-A board. A schematic diagram of the modifications can be seen in Figure 16.

The stimulator was set for a pulse width of 50 us and was triggered through DAC channel 0 of the DT-2801-A board. Stimulation amplitude is voltage controlled through a BNC panel jack on the front panel which was connected to DAC channel 1 of the DT-2801-A board. A switch selects between manual and external computer control of the stimulus amplitude.

2.4.2 STIMULATION ELECTRODES

One stimulating electrode was a one inch by one inch flat lead surface electrode that was placed under the palm of the subject's hand. The other electrode was a 6 mm diameter disc placed over the end plate zone of the FDI. The small disc electrode was moved around the surface of the skin above the

Figure 16

Stimulator Modifications

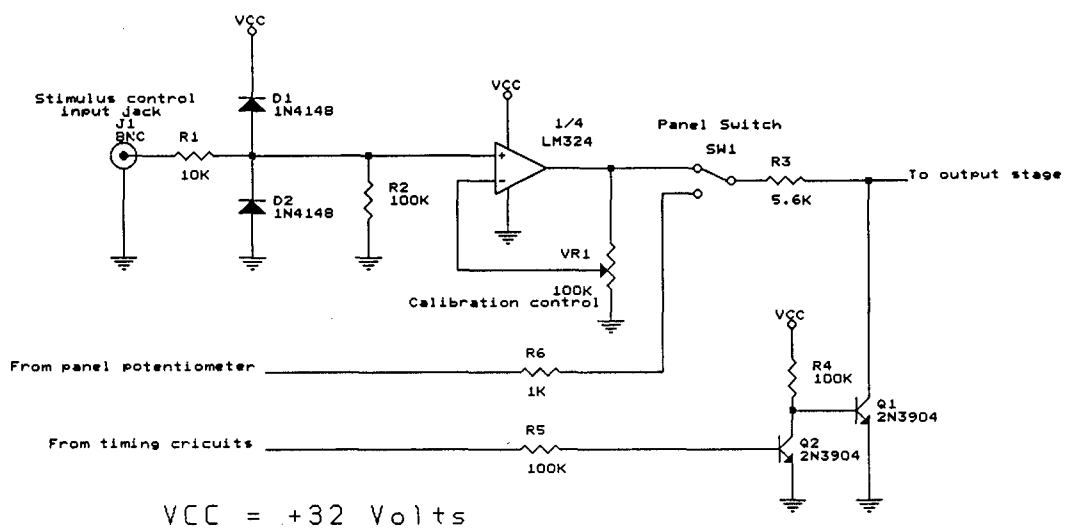

FDI to find the place where the stimulation produced the greatest visible muscular reaction with the least amount of pain to the subject. This placement was considered closest to the end plate zone. The small disc electrode was then taped over the end plate zone. Moving the disc electrode changed the MU recruitment order (see Section 4.6) and provided opportunity to investigate different MU recruitment orders than achieved with the single disc electrode placement over the end plate zone.

The small disc electrode was intended to produce a large current density over the end plate zone, while the large surface electrode at the palm provided a return path for the current with a low enough current density so that no muscles near the palm were stimulated. This stimulating electrode configuration was found to provide good stimulation selectivity and caused only a moderate amount of pain to the subject for large stimulations.

If the small disc electrode was incorrectly placed, or the current density near the large electrode was too high, other muscles besides the FDI may twitch from stimulation. In turn, the EPLA measurement could be affected. The effect of inadvertent stimulation of other muscles is discussed in Section 1.6 and Section 2.3.6.

2.5.1 COMPUTER TYPE

The computer used in this thesis was a 286 AST machine with an 80287 coprocessor chip running at 10 Mhz. It had 640K ram, an EGA graphics board and a 40 Mbyte hard disk drive along with 1.2 Mbyte and 1.44 Mbyte removable disk drives. It contained a Data Translation DT-2801-A analog and digital I/O board. The board was plugged into one of the computer expansion slots and provided A/D and D/A capabilities with 12 bits of resolution. For A/D conversions, 16 single ended channels or 8 differential channels could be monitored. The board contained two D/A channels. The A/D throughput was programmable up to 27.5 Khz. The board also provided two 8-bit digital I/O ports which were not used.

Detailed information about the analog to digital and digital to analog conversion and other capabilities of the DT-2801-A board can be found in the Data Translation DT-2801-A Manual. (Data Translation Inc., 1983)

2.5.2 HARDWARE CONNECTIONS

The DT-2801-A board was configured for 8 differential input channels to minimize the 60 Hz interference in the cables leading to the DT-2801-A board. All of the A/D channels were configured for +/-10 volts operation. The

accelerometer amplifier output was connected to A/D channel 0. The A/D channels are 12 bits, giving a resolution of 49 mV. The acceleration DC signal was set to -7.5 volts (see Section 2.2.4). Since positive peak acceleration was of primary interest (see Section 1.7), the offset increased the dynamic range of the measurement of the positive peak acceleration.

The DAC channels were configured for 0 to +10 volt operation. DAC channel 0 controlled the stimulus trigger by changing level from 0 to +5 volts. The rise time of the DAC output was not sufficient to trigger the stimulator, so a digital buffer with hysteresis was needed between the DAC channel 0 and the stimulator trigger signal. This buffer was put inside the case of the accelerometer amplifier and powered by the accelerometer power supply.

DAC channel 1 controlled the stimulus amplitude of the stimulator through the modifications described in Section 2.4.1 giving a stimulus resolution of between 24.4 mV and 97.7 mV, depending on the output scale of the stimulator.

CHAPTER 3.

SOFTWARE

3.1 BRIEF OVERVIEW

Three pieces of software were written specifically for this thesis: A program for the simulation of electrical muscle stimulation, a sophisticated program to control the computer hardware previously described in Chapter 2 to record force data from muscles in the manner described in Section 2.2.2, and a program for the nearest neighbour classification of data recorded by the twitch recording software.

3.2 MUSCLE RESPONSE SIMULATION

First, a program called ALT.M was designed for use in the development software MATLAB for the simulation of electrical muscle stimulation. It simulated the action of the activation curve of MU firing which can be referred to in Section 1.5. Since the addition of MU force is linear, the total muscular force is the sum of the individual MU forces. Dynamic control of stimulus amplitude was not simulated, but provision for adding dynamic stimulus control was incorporated. The results of several simulations is shown in Section 4.1.

3.3.1 TWITCH RECORDING SOFTWARE

The second program, TWITCH.C, was written for Borland Turbo C++ and when used with the hardware described in Chapter 2, provides semi-automation of the recording of a number of EPLA responses. Only the first 37.5 milliseconds of the lateral finger acceleration was measured for each twitch because the EPLA typically occurs within 25 milliseconds of stimulation. More details about peak muscular force and EPLA can be found in Section 1.7. The entire twitch recording software operates as follows:

1) Check to see if the program usage was correct
2) Prompt the user to choose filtering options:
    a) No filtering
    b) Optimal filtering:
        1) Read in 500 points at 1Khz of acceleration data
            a) Find mean and standard deviation of baseline noise
        2) Set up the user graphics screen
        3) Wait for 50 points at 1Khz within 2 standard deviations of base noise
        4) Check the keyboard for changes in operation
        5) Set up the DT-2801-A to record 37.5 ms at 4 Khz
        6) Read acceleration data from AD channel 0
        7) Compile twitch shape for optimal filtering

8) Update the screen with the new twitch data

9) Adjust stimulus amplitude as necessary

10) Return to step 3) until 100 responses averaged

3) Prompt the user to choose type of data recorded:

a) Modify stimulus to record responses near a force level

b) Modify stimulus to record desired ramp in force

c) True Ramped stimulus

4) Open output files

5) Put the computer into EGA graphics mode

6) Reset the Data Translation DT-2801-A board

7) Read in 500 points at 1Khz of acceleration:

a) Find mean and standard deviation of base noise

8) Set up the user graphics screen

9) Wait for 50 points at 1Khz within 2 standard deviations

10) Set up the DT-2801-A to record 37.5 ms at 4 Khz

11) Stimulate the subject with appropriate amplitude

12) Read acceleration data from AD channel 0

13) Perform filtering options if necessary

14) Update the screen with the new twitch data

15) Save the following data to file if not clipped:

a) Number of milliseconds to maximum acceleration

b) AD value of maximum acceleration

c) Optimally filtered acceleration amplitude

d) Stimulus amplitude

e) Area under acceleration trace (Momentum)

f) Time of occurrence of stimulation

16) Adjust stimulus amplitude as necessary

17) Return to step 9) until all responses recorded

Some of the operational steps of the program TWITCH.C are self-explanatory. The following chapters provide a detailed description of the steps that require further explanation.

3.3.2 INPUT ARGUMENTS

The program TWITCH.C was not executable before compilation by Borland's Turbo C++ compiler. It had to be compiled with the huge memory model and the graphic libraries had to be attached. After compilation, the program TWITCH.EXE was executed by typing:

TWITCH <Filename> <Number of stimulations>

If the input arguments were not correct, a message was displayed and the program terminated. During execution, the program could be terminated at any time by pressing the <END> key.

3.3.3 OPTIMAL FILTERING

In Section 1.7 it is stated that twitch acceleration shape is primarily determined by the dynamic properties of the

subject's index finger. If those properties do not change significantly during subject testing, and if those properties are linear, then the twitch acceleration shape would be constant and EPLA would then be proportional to peak muscular force. If the shape and timing of any transient signal is known, a technique called weighted pulse sampling (Wilmshurst, 1985) could be used to determine the amplitude of a noise record of that signal.

Figure 17 shows a typical acceleration trace and the method of applying weighted pulse averaging to determine pulse amplitude. The integrator must be reset before the application of each pulse. Incoming samples are multiplied by a shape function that has the same shape as the incoming pulse. The multiplied signal is then integrated and the integrated signal will settle to a value proportional to the incoming pulse amplitude. The timing of the shape function and the incoming pulse must be exactly matched.

The timing of the twitch was easily related to the timing of the stimulus because the twitch was evoked by the stimulus. Twitch shape was approximated by averaging the normalized responses of 100 twitches. For the purposes of optimal filtering, the actual twitch shape was then assumed to be

Figure 17
Optimal Filtering Technique

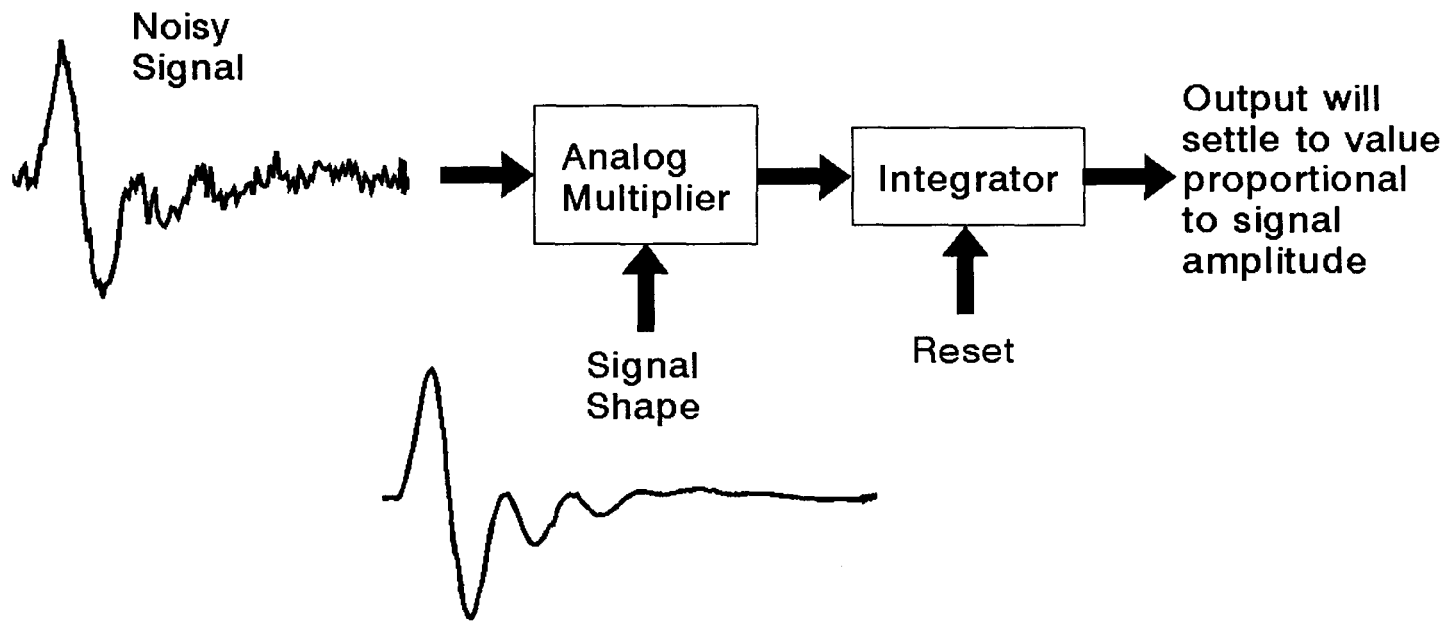

1) Noisy signal and signal shape must have same timing
2) Integrator must be reset before each pulse
3) Output value is proportional to pulse amplitude

equal to the normalized average twitch shape.

The signal to noise ratio of the estimated twitch shape is increased from that of a typical acceleration response by a factor of the square root of N by the signal averaging (Clark et al., 1992), where N is the number of responses averaged. Although the twitch shape used for optimal filtering was not exact or of infinite signal-to-noise ratio, some reduction of EPLA error may be possible using a twitch shape approximation for the optimal filtering procedure. Further reduction of EPLA error may be possible using a better twitch shape. A Section 4.3.7 discusses the effectiveness of this method of filtering.

3.3.4 STIMULUS CONTROL

The hardware of the stimulus amplitude control is described in Sections 2.4.1 and 2.4.2. The software control for the semi-automation of stimulus amplitude will now be briefly described. The program TWITCH.C is programmed with a desired EPLA and upon stimulation, compared the actual EPLA with the desired EPLA. The desired EPLA is chosen by the user for EPLA responses within the input range of the A/D board. If the actual EPLA was lower than the desired EPLA, the stimulus amplitude for the next stimulation was increased.

Conversely, if the actual EPLA was higher than the desired EPLA, the stimulus amplitude for the next stimulation was decreased. The stimulus amplitude of the following stimulation was changed by a linear combination of the amplitude error, the AD clipping level, the signal baseline and a stimulus control sensitivity parameter. The sensitivity parameter of the stimulus control can be modified during the program execution by the operator for additional stimulus control.

When the user instructs the computer to record twitches in the constant amplitude mode, the desired EPLA remains constant for the number of stimulations defined by the user. During program execution the user was able to adjust the desired EPLA if necessary.

When the user instructs the computer to record a ramp in force, the desired twitch maximum is graded from the first to the last stimulation. In this case, the desired twitch maximum increases as the stimulation number increases. The user still maintains the ability to override the computer's control of the desired twitch maximum during program execution through the keyboard interface.

3.3.5 KEYBOARD INTERFACE

During the execution of the program TWITCH.C, there were several ways for the user to modify program operation. A complete description follows:

KEY	ACTION
<END>	Terminates program operation
<UP ARROW>	Increases desired EPLA
<DOWN ARROW>	Decreases desired EPLA
<PAGE UP>	Increases force control sensitivity
<PAGE DOWN>	Decreases force control sensitivity
<HOME>	Pauses program operation

Any other key continues

3.3.6 GRAPHIC INTERFACE

The graphics of the program provided the user with feedback of the information recorded and allowed the user to intelligently modify the program operation during program execution.

Figure 18 shows a typical graphic screen during program execution. The top half of the screen contains an EPLA plot. Two small indicator lines at the extreme right and left of the screen show the user the desired EPLA. Clipped responses are

Figure 18

Twitch Recording Software
Graphic Interface

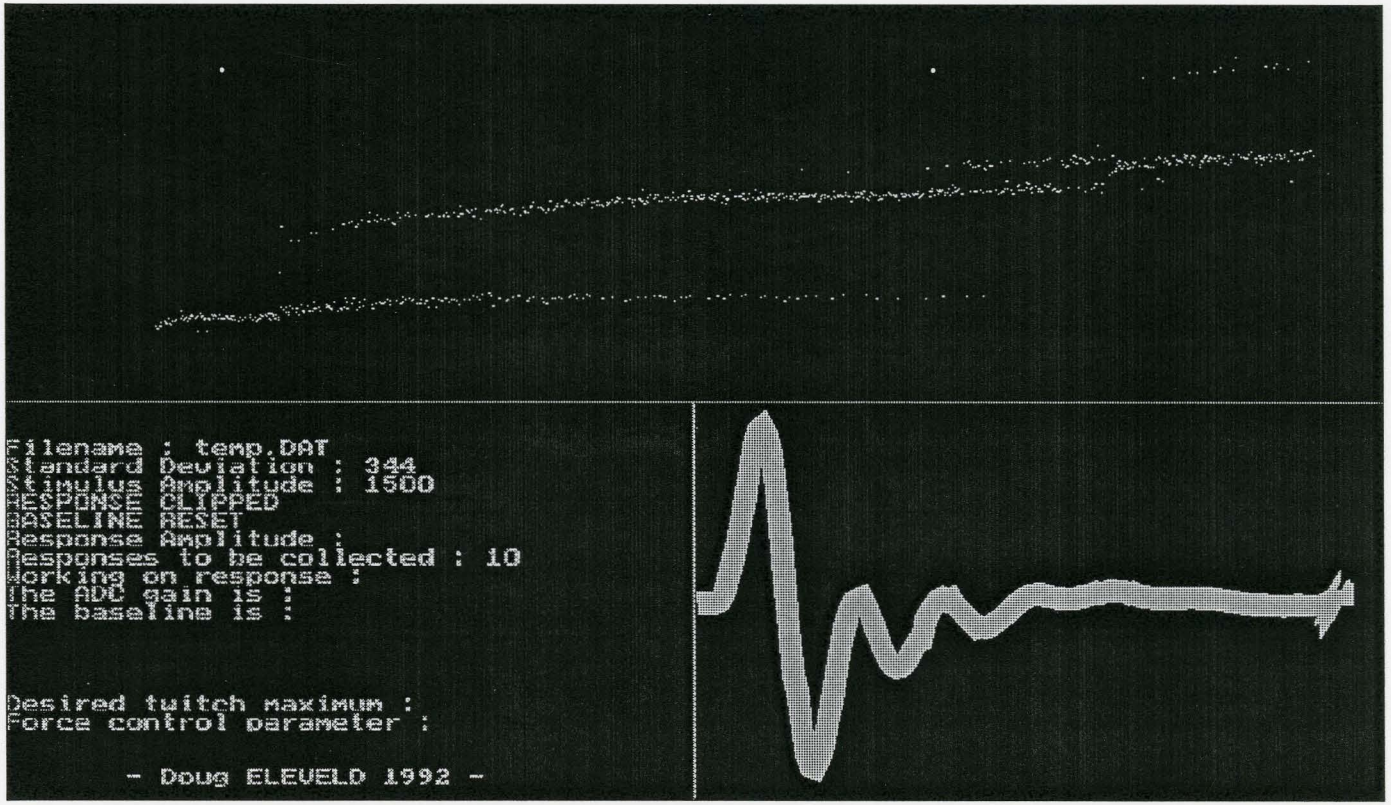

plotted in a different colour than valid responses and the clipped responses are not saved to the data files. The bottom right of the screen contains a normalized plot of the twitch record gathered. It shows 37.5 milliseconds of acceleration data after stimulation and is updated after every stimulation. This section of the screen gives the user immediate feedback of the acceleration twitches gathered. The bottom left of the screen contains text indicating the operation of the program which include:

1) Output filename
2) Baseline noise standard deviation
3) Stimulus amplitude *
4) If the last response was clipped *
5) If the baseline was reset on the last stimulation *
6) Response amplitude *
7) Number of responses to be collected
8) Current response number *
9) The ADC gain of the DT-2801-A board
10) The baseline value *
11) The desired twitch maximum *
12) The force control sensitivity parameter *
13) Program author and date

The information marked with * is updated after every stimulation.

3.3.7 OUTPUT FILE FORMAT

The program TWITCH.C outputted 2 different ASCII files which contained the following data:

1) Number of milliseconds to maximum acceleration
2) A/D value of maximum acceleration
3) Optimally filtered acceleration amplitude
4) Stimulus amplitude
5) Area under acceleration trace (Momentum)
6) Time of occurrence of stimulation

The file with the extension .DAT contains the data for each stimulation on one line with each field separated by commas. This file format can be easily read into programs such as MATLAB. In MATLAB, data analysis and plotting were done easily and quickly. Another file with the extension .NN was used with a program called NN.C. This program performs nearest neighbour clustering analysis of the data recorded by TWITCH.C. A complete explanation of the NN.C program can be found in the Section 3.4.1.

3.4.1 DATA CLUSTERING SOFTWARE

Finally, a program to evaluate the clustering of data

recorded by TWITCH.C called NN.C was devised. This program was written in Borland Turbo C++ and must be compiled with a huge memory model. Also, graphic libraries must be attached. An overview of the program protocol is as follows:

1) Check to see if program usage is correct
2) Verify relevant data to user
3) Read in data file *.NN
4) Plot data points on graphics screen
   - Plot any variable against any other variable as determined by definitions in NN.C
5) Connect points within user defined ellipses to form clusters
6) The means of all the clusters are calculated
7) The user is shown the means of all the clusters
8) A file is saved containing the cluster information

While the clustering was in progress, a bar across the bottom of the screen gave the user an idea of how long the clustering will take, and how much clustering had already been done. At any time during the clustering, the <END> key could be hit to immediately terminate the program. If clustering analysis is desired on a subset of the points in the data file, then the appropriate data points must be removed from the file using a text editor.

3.4.2 INPUT ARGUMENTS

The program NN.C cannot be executed before compilation by Borland's Turbo C++ compiler. After compilation, the program NN.EXE was executed by typing:

NN <Filename> <X threshold> <Y threshold>

The X and Y threshold variables determined the degree of clustering that was done. Points were clustered together if they were within an ellipse with dimensions determined by the X and Y thresholds. The ellipse is calculated using a simple euclidian distance calculation. The thresholds are chosen heuristically so that the clustering results reflect user judgement about the clusters existing in the data. If the input arguments were not correct, a message was displayed and the program terminated.

3.4.3 CLUSTERING METHOD

The muscle being studied can be considered a single-input, single-output system. The relative peak force production of the muscle is the output and stimulus amplitude is the input, although other variables may be chosen with simple program modifications. The transfer function then becomes the plot of relative peak force production versus stimulus amplitude.

Clusters in the transfer function graph are indicative of the presence of discrete MUs. Quantitative evaluation of the placement of the clusters was necessary for estimation of MU EPLA contribution. The clustering method for the program NN.C is as follows:

1) User supplies clustering thresholds
2) All data points within an ellipse (or circle), with dimensions determined by the thresholds are clustered together
3) Data concerning the cluster positions and particular data points in each cluster were output to file

3.4.4 GRAPHIC INTERFACE

Graphics were included in the NN.C clustering program to give the user quick visual feedback about the validity of the clustering thresholds supplied. This allows the user to adjust the thresholds and cluster the data again.

Figure 19 shows a typical graphic screen during program execution. The graphic screen contains a plot of the transfer function of the muscular system. The X-axis was chosen as stimulus amplitude and the Y-axis as EPLA. The data points are in white and points in the same cluster are joined by green lines.

Figure 19

Data Clustering Software
Graphic Interface

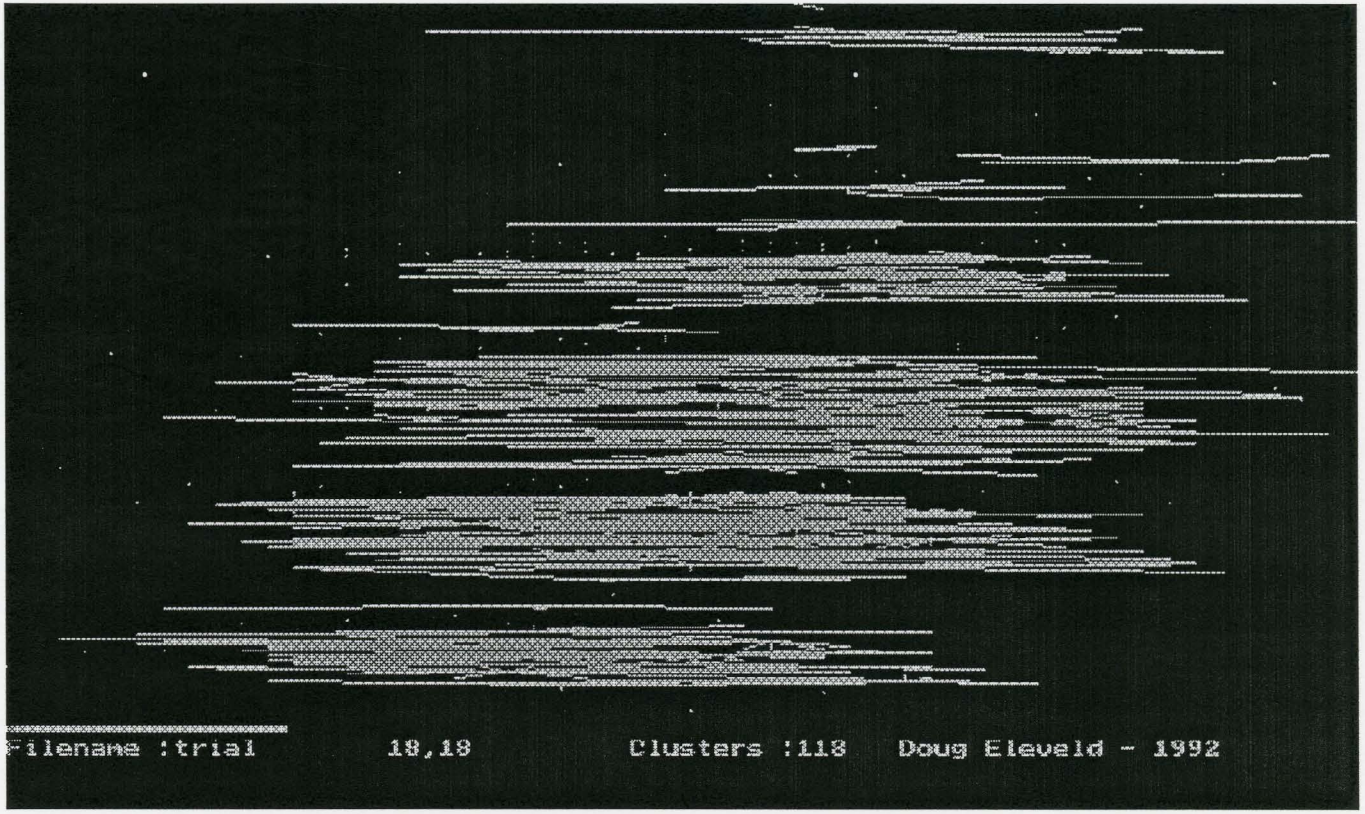

The bottom of the screen contains text indicating the operation and setting of the program. The information displayed in this section is:

1) Filename
2) Clustering thresholds
3) Current number of clusters
4) Progress bar graph

3.4.5 OUTPUT FILE FORMAT

The program NN.C outputted an ASCII file which contained the following data:

1) Filename
2) Clustering thresholds
3) Cluster numbers
4) The number of points in each cluster
5) The means of each cluster
6) All data points and the corresponding cluster number

This file has the extension .MEA. It was designed primarily for ease of reading by the user. With some simple changes with a text editor, the file can be easily read into programs such as MATLAB. In MATLAB, data analysis and plotting are done easily and quickly.

CHAPTER 4.

RESULTS

4.1 SIMULATION RESULTS

Figure 20 shows a simulation of a number of EPLAs of a human muscle. EPLA is plotted against stimulation number. Stimulation amplitude was ramped to invoke the firing of several MUs. No alternation was simulated. Also, there was no Gaussian random noise added. Solid lines indicate the force contribution of MU in non-alternated order.

We can see clusters of EPLA responses along the lines in Figure 20 and the distance between these bands is equal to the amplitude of the force production of the MU. Graphs similar to Figure 20 have been achieved by Veltink et al. (1989) using intrafasicular multielectrodes on rat tibialis anterior and extensor digitorum longus muscles.

Figure 21 shows a simulation of the effect of Gaussian random noise added to the force value. This models the effect of noise contributors discussed in Section 2.3.1.

Figure 20

No Alternation, No noise

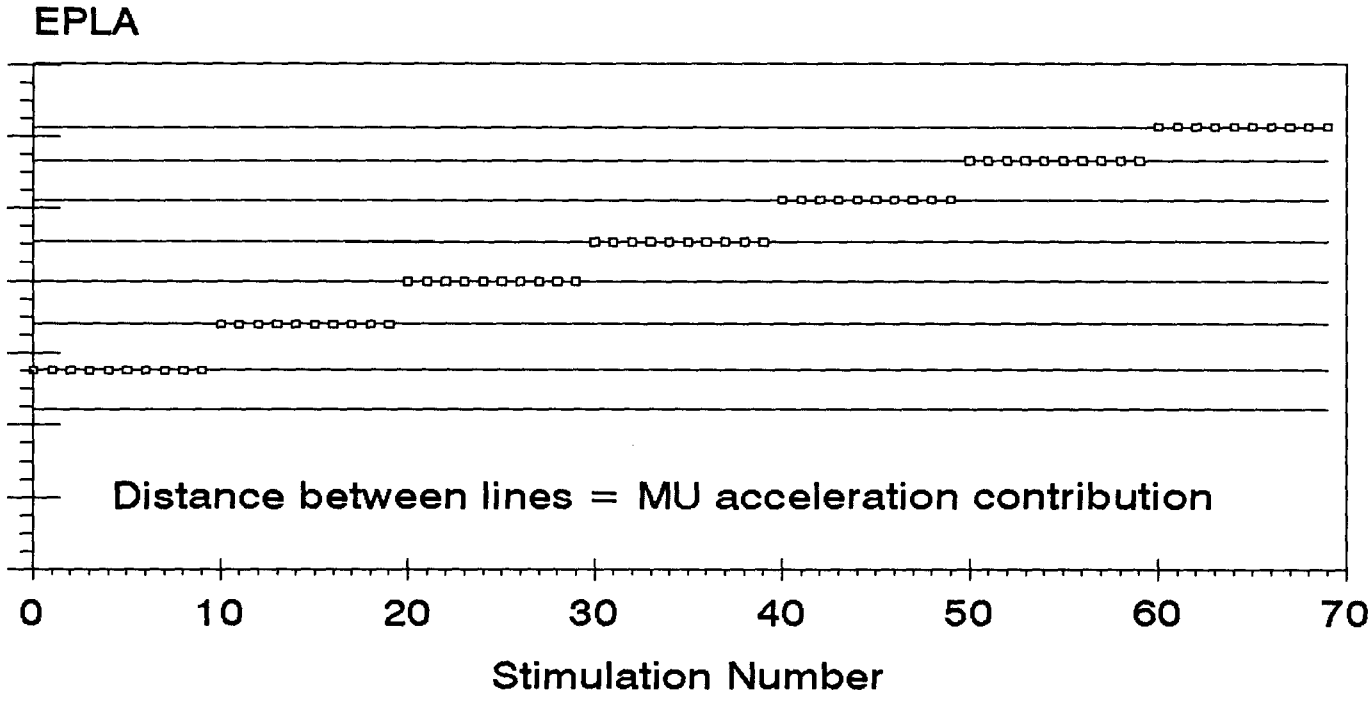

Simulation #1

Figure 21

No Alternation, Some noise

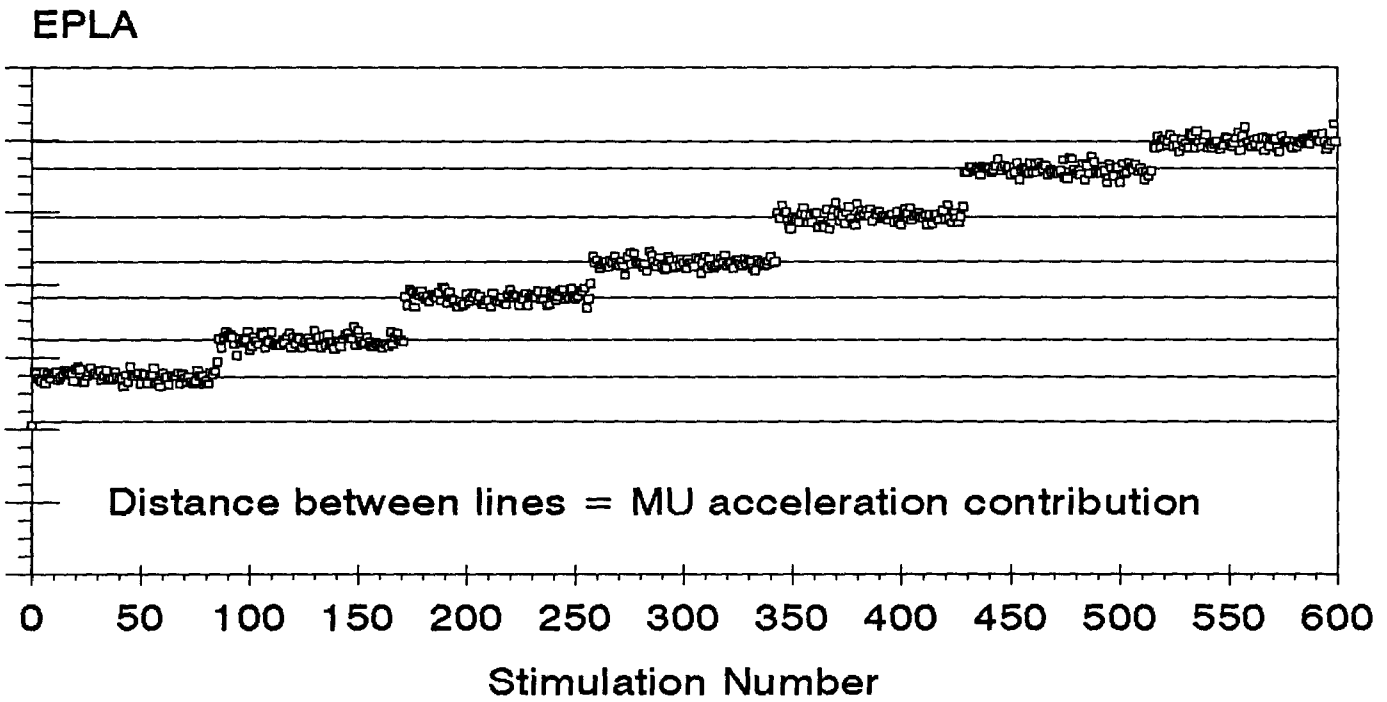

Simulation #2

It is evident in Figure 21 that the noise sources cause spreading or blurring of the force lines into bands. If there was excessive noise, the bands spread so much into each other that the bands were not separable. This occurred if the ratio of noise to MU size became high. Large MUs would be discernable, but smaller MUs would not be, thus there is a lower limit to detectable MU sizes.

Figure 22 shows a simulation with no Gaussian noise and moderate alternation.

It is evident that the effect of alternation was to produce less dense sub-bands between the major bands. The less dense bands correspond to alternated responses. The distance between major bands is proportional to the size of the MU. The distance between major and minor bands is proportional to the difference between the alternated and non-alternated responses. The density or number of points in a band is related to the probability of the alternated response that the band represents. For example, a very dense band would be a non-alternated response. A slightly less dense band would be a slightly less likely alternated response. One or two points at a particular force level, that is to say, an almost empty band, would correspond to an unlikely alternated response. The density of the bands is related to the

Figure 22

Alternation, No noise

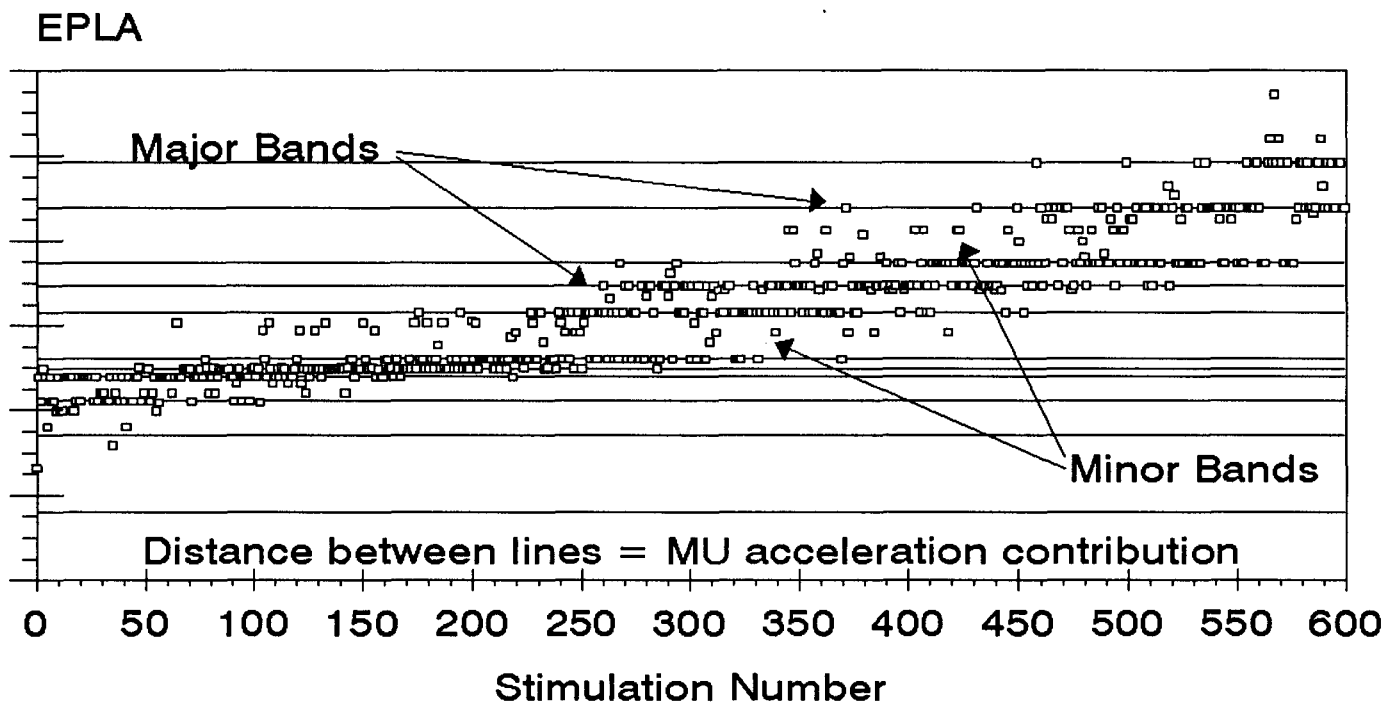

Simulation #3

probability of that particular force level being produced, and this is of decreasing likelihood for lower probability alternated responses.

Bands that are near the upper an lower extremes of the EPLA simulation are low density bands because the range of stimulus amplitudes used for that particular simulation were not high enough to consistently excite those MUs, not because they are alternated responses. Therefore, if a low density band exists between two higher density bands, then the low density band is an alternated response. If the low density band is not surrounded by higher density bands, then the low density of that band is the result of that MU not being stimulated frequently with the range of stimulus amplitudes used for that simulation.

There are some conditions where the general rule of alternation producing more low density bands between higher density bands may be misinterpreted. Figure 23 shows one of these conditions.

Figure 23 was produced by the simulation program ALT.M where the MUs were nearly the same size and much alternation occurred. The alternated bands for similarly sized MUs tended to be closely positioned to a non-alternated band and may be

Figure 23

Alternation, Similar MU sizes

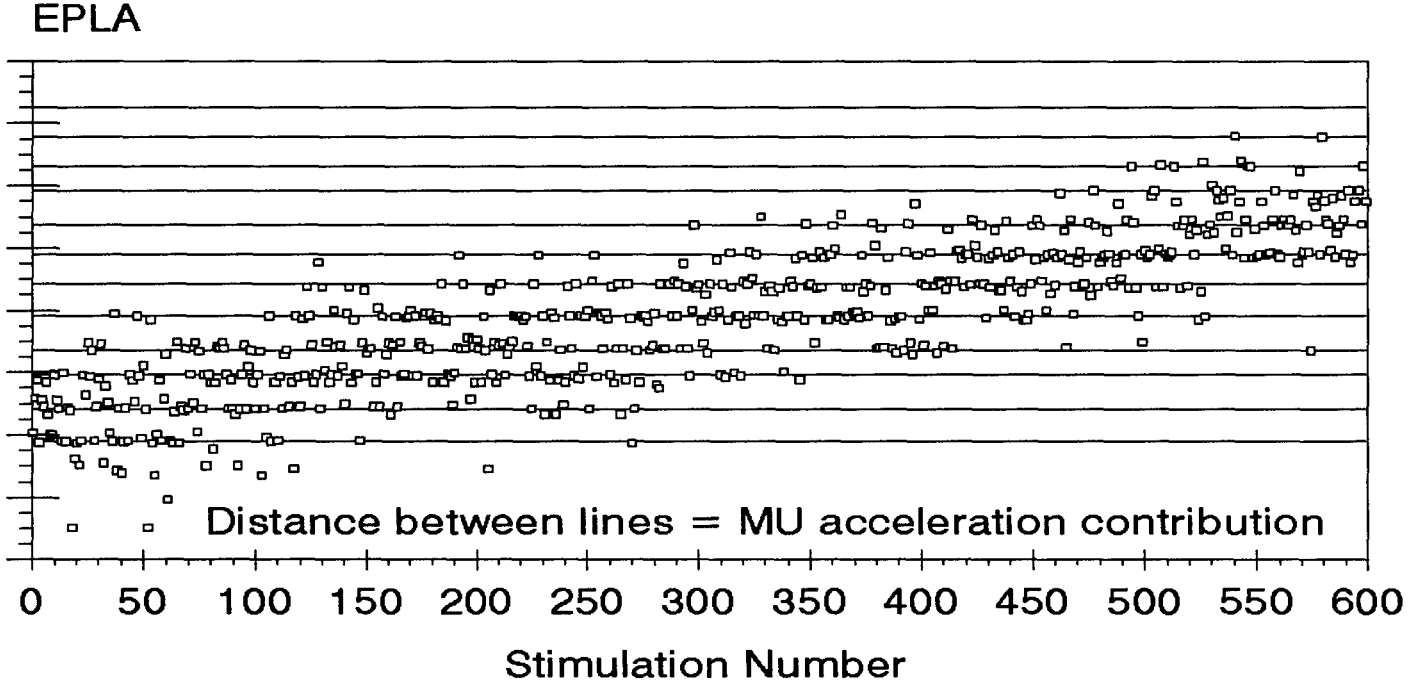

Simulation #4

interpreted as being part of that band. Excess noise would further cloud the differentiation of the alternated and non-alternated responses. Since the less likely alternated responses are also nearly equal to the non-alternated response band, the non-alternated response band may be interpreted as a noisy band, and the mean of the band may be shifted. The mean of the band is shifted towards the mean of the MUs that are alternating with the MU in question. So, in this case the distance between bands is no longer equal to the MU EPLA contribution, but is proportional to the weighted average of the MU EPLA with other MUs having similar stimulation thresholds. This affects the individual MU EPLA contribution calculation, but it does not affect the validity of average estimates of MU EPLA contributions.

In the extreme case, all MUs are exactly the same size and alternated responses would fall exactly on the non-alternated response bands. The degree of alternation then becomes irrelevant and MU estimation becomes very easy. This extreme case is simulated in Figure 24.

4.2.1 PRACTICAL CONSIDERATIONS

The force production of a MU is dependent on many variables. Of particular interest in this thesis is the

Figure 24

Alternation, Same MU sizes

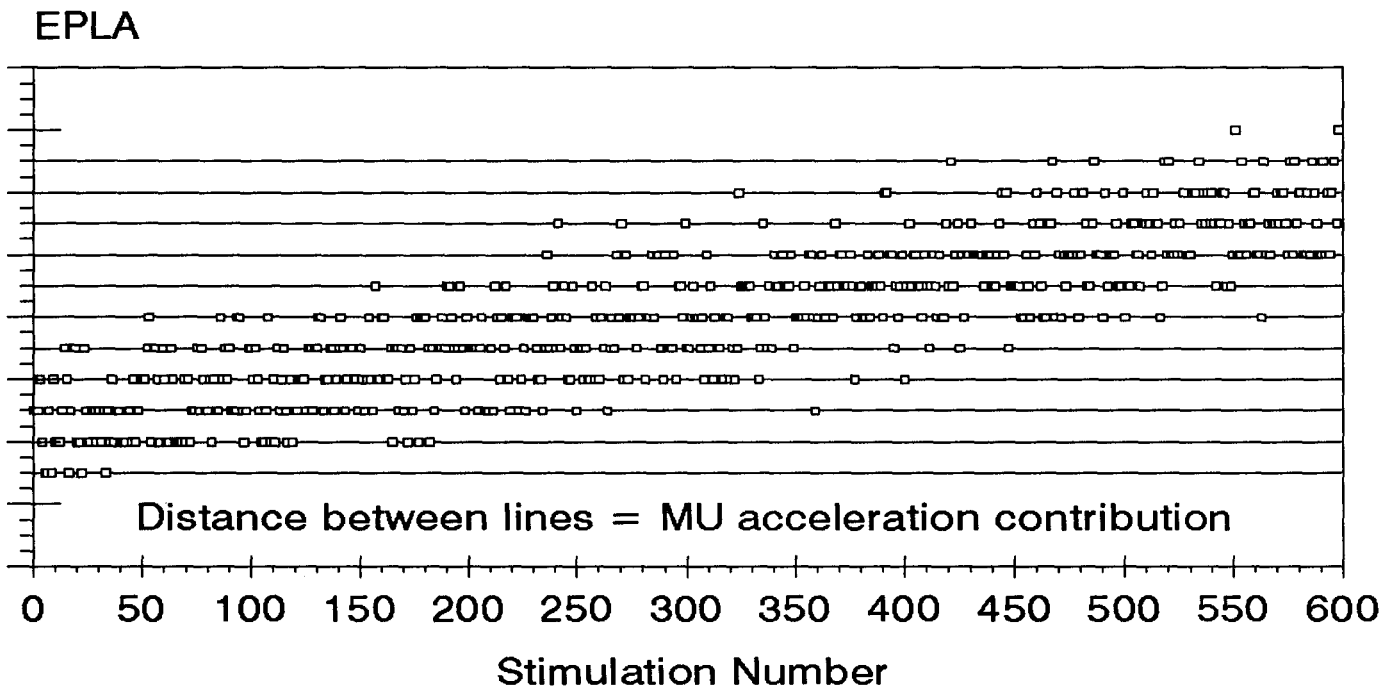

Simulation #5

number and strength of muscle fibres innervated by the motor neuron and its past firing history. MUs with many muscle fibres will produce large peak forces and MUs with few muscle fibres will produce relatively small peak forces. Muscle fibres that are stimulated at 1-3 Hz may exhibit twitch potentiation, which is also known as the staircase phenomenon. Both twitch potentiation and the number of muscle fibres in each motor unit need to be discussed before investigating data collected from human muscles.

4.2.2 TWITCH POTENTIATION

The peak force production of a MU is dependant on the past history of MU firings. If a MU is excited by a high frequency for a long period of time, it will fatigue and its peak force production will drop. The fatigue resistance varies greatly between different MUs depending on their biochemical energy source.

If a MU is stimulated at about 1-3 Hz, its force will increase to a new maximum. This is known as twitch potentiation or the staircase effect. (Desmedt and Hainaut, 1968) The software TWITCH.C used in this thesis stimulated the subject as fast as possible without causing twitch fusion, which occurs at about 3-4 Hz. Therefore, changes in MU EPLA

contribution due to twitch potentiation was apparent in the data recorded by that software and must be taken into account in the data analysis.

The technique of spike triggered averaging (Milner-Brown et al., 1973) involves triggering a force averager with the EMG of a single MU recorded with a bipolar needle electrode. Typically, several hundred responses are averaged for each unit. If the MU used for triggering potentiates, then the averaged result will have a larger magnitude than the real MU unpotentaited twitch.

Section 4.3.5 investigates the typical magnitude of MU force potentiation for a trial run on a typical human subject.

4.2.3 EFFECTIVE FIRING FREQUENCY

At a particular stimulus amplitude, there are several MUs that may be stimulated. If this stimulus is continued for a long time, some MUs will fire more frequently than others. For example, if a subset of MUs is stimulated many times, some MUs will always be firing, some MUs will never fire, and some MUs will fire at varying probabilities. If a muscle is stimulated at 4 Hz and at a stimulus intensity such that a particular MU fires with a probability of 0.25, then that MU

effectively fires at 1 Hz. The effective firing frequency will determine whether or not the MU will exhibit twitch potentiation. Therefore, it is important not to compare the force contributions of different MUs that are firing at different effective frequencies. This point has great implications as to when the MELA should be determined, and what data sets contain valid information regarding MU EPLA contributions. MU EPLA contributions should be obtained as closely as possible in time to the MELA test so that MELA contribution matches MU EPLA contribution as closely as possible. This ensures that the MU exhibits the same amount of potentiation in the MELA test as in the MU EPLA contribution tests. For the best MU number estimates, it does not matter whether the MUs are potentiated or not provided than the MUs have the same amount of potentiation in the MELA and MU EPLA contribution tests.

4.2.4 TEST ORDER

As a muscle is repetitively stimulated, some of the MUs may have effective firing frequencies within the range of frequencies pertaining to twitch potentiation. Those MUs will change their force contribution over time which may smear or skew the bands in the EPLA vs stimulus number graph. Therefore, for maximum clarity of smaller MU force

productions, the MELA data for the muscle should be recorded before attempting to repeatedly stimulate the smaller MUs to try to ensure static potentiation conditions. Also, the force contribution of a MU should be determined at a time close to the determining of the MELA. In this way, the MUs contribution to MELA can be most accurately determined.

4.3.1 TRIAL RUN

With the results of the simulations and our discussions about practical considerations in mind, let us examine some data for real human muscle collected using the hardware described in Chapter 2 and the software described in Chapter 3. The results of using several different collection modes will be described in several sections.

4.3.2 MOTOR UNIT SEPARATION

Figure 25 shows a trial run that used the constant force gathering mode of the program TWITCH.C, the hardware described in Chapter 2, and the stimulation methods described in Chapter 1. In the constant force gathering mode of TWITCH.C, the stimulus amplitude was controlled to obtain a pre-determined EPLA. Alternation and varying thresholds of MUs made recording exactly similar EPLAs for different stimulations

Figure 25

Trial Run 1

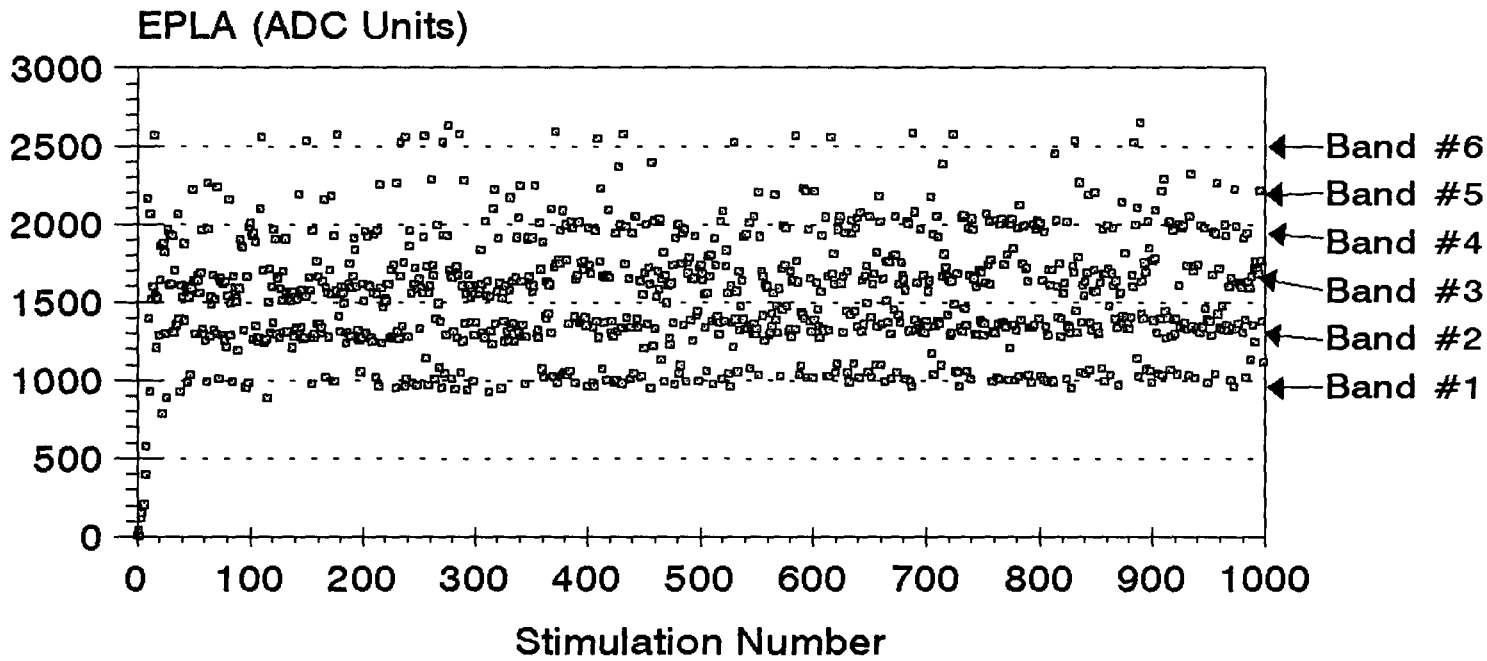

Constant acceleration mode
EPLA gain = 28573

impossible, thus a range of accelerations were recorded. Amplifier gain setting for this run was 28573.

Bands in this graph are seen just as predicted from simulation (see Section 4.1) using the ALT.M program and are similar to graphs obtained by Veltink et al. (1989) for rat tibialis anterior and extensor digitorum longus muscle using intrafasicular multielectrodes. However, Figure 25 was obtained with FDI motor point stimulation and EPLA measurements. Veltink et al. were unable to produce graphs containing bands using extraneural stimulation even though their force measurements were made with the tendons of the muscle directly connected to force transducers. It is shown in Figure 25 that bands in the force response of human muscle can be produced while analyzing EPLA with motor point stimulation and without the disruption of the muscle tendons or nerves.

No filtering was performed to the acceleration signal before extracting the peak amplitudes. This particular run had six approximately evenly spaced bands. This indicates that there may be four or five similarly sized MUs present. Bands 5 and 6 are low density clusters, however they do not correspond to alternated responses. These bands correspond to real MUs because of their placement at an extreme of the force

levels gathered. The range of stimulus amplitudes used in this particular trial run were not high enough to excite those MUs frequently. The first few EPLA responses were much lower than the rest. This was because at the initiation of the trial run, the stimulus amplitude was set too low for excitation of the desired MUs. The computer control of stimulus amplitude increases the stimulus amplitude until the EPLA responses are near the desired EPLA response. Desired EPLA response is chosen for EPLA responses within the input range of the A/D board. Details of the stimulus amplitude control can be found in Section 3.3.4.

It is important to note that these MUs do not have the lowest stimulation thresholds in the muscle, and bands corresponding to the first MUs recruited for increasing stimulus intensity are not shown. Some MUs are excited at every stimulation, and consequently no points in Figure 25 correspond to those MUs. Investigating those MUs requires setting the desired EPLA of the twitch gathering software lower. This can be easily done during program execution. (see Section 3.3.4)

The accelerations measured must only be considered relative to peak MU force. (see Section 1.7) Therefore the units of acceleration are not important for data analysis.

For all trial runs in this thesis, the units of acceleration are the values read from the analog to digital conversion (ADC units) card in the computer. Relative MU EPLA contributions and estimations of number of MUs in a subject's FDI can be calculated using ADC units.

4.3.3 TRANSFER FUNCTION

To fully evaluate the source of the bands in Figure 25, it is necessary to look at the muscular system transfer function. For this system, the input is the stimulus amplitude and the output is the EPLA. Figure 26 shows this transfer function. Only points numbered 100 to 1000 from Figure 25 were included in the transfer function graph.

It is conceivable that the bands in Figure 25 could be the result of the computer control 'missing' some stimulus amplitudes. However, the clusters in the transfer function show that no stimulus amplitudes have been 'missed' and that the bands in Figure 25 are truly the result of muscular properties. In this case, the all-or-nothing response of human skeletal MUs produces the bands.

The limited resolution of the stimulus amplitude control can be easily seen in Figure 26. It is also evident that the

Figure 26
Transfer Function

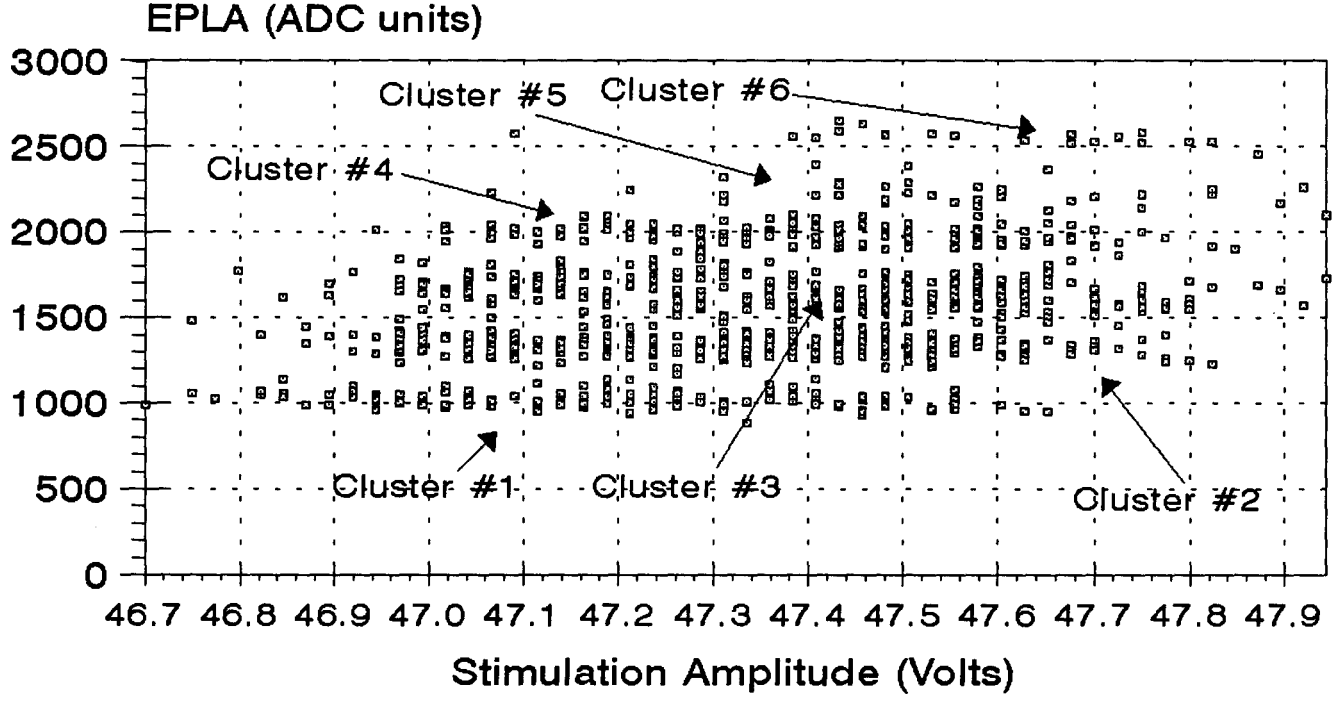

Transfer function of data from Figure 25

variance of threshold for any MU varies over a wide enough range that the existing resolution of the stimulus amplitude is adequate to show the basic firing properties of these MUs.

4.3.4 NOISE EVALUATION

The spread of the bands could be due to noise sources or alternation from similarly sized MUs. (see Section 4.1) To evaluate the source of the band spread, the probability distribution of a cluster of points was evaluated. The program NN.C was used for clustering analysis. Figure 27 shows an approximation of the probability distribution of band 2 from Figure 25, which can also be seen as cluster #2 in Figure 26. The clustering thresholds were determined empirically to separate the major clusters in the data. Clustering was limited to points 100 to 1000 from cluster #2 in Figure 25.

The distribution shown in Figure 27 appears to be Gaussian and uni-modal. If the distribution was bi-modal, then the cluster probably contains two responses, probably a non-alternated and an alternated response. If the cluster was bi-modal, then the two distributions may be separated by lowering the clustering thresholds. Because the distribution of Figure 27 is Gaussian and uni-modal, it is probably the

Figure 27
Noise Evaluation

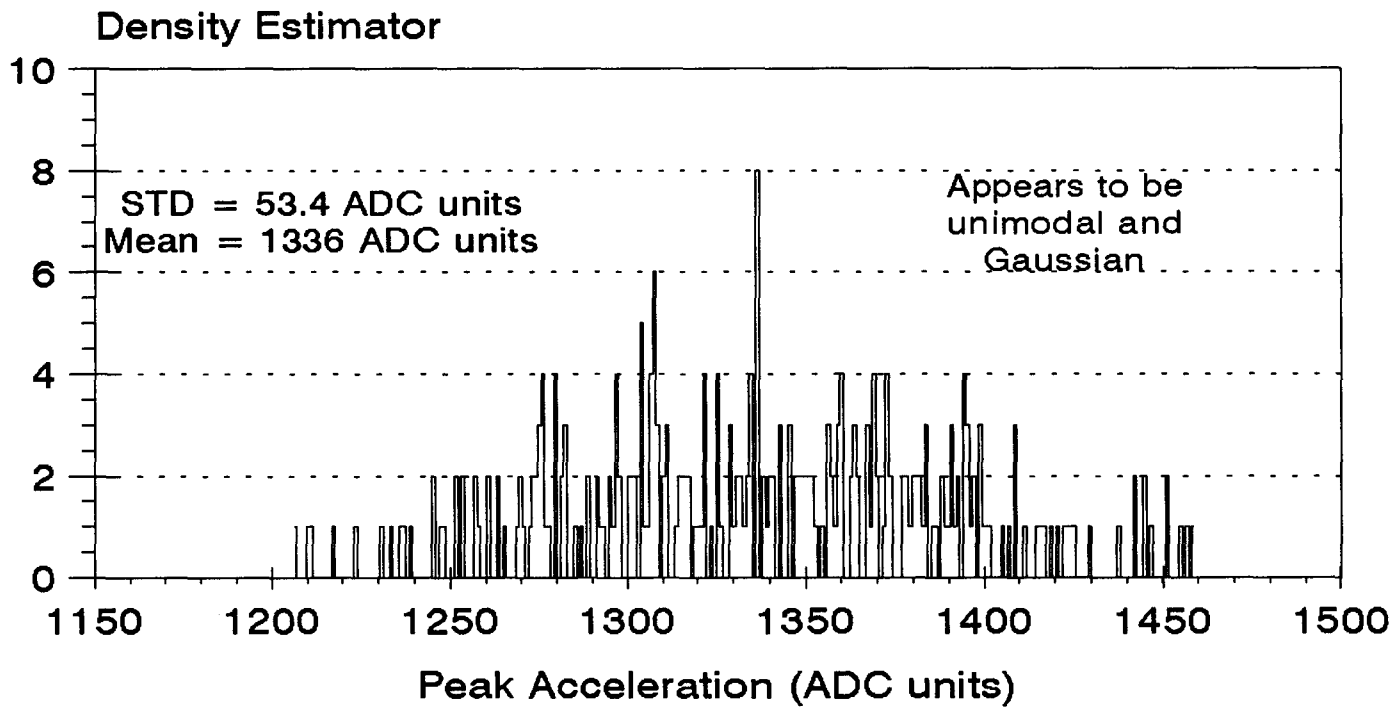

Cluster #2 from Figure 26

result of the contribution of one MU to the EPLA.

The standard deviation of the noise is 53.4 ADC units, and the mean of the cluster is 1336 ADC units. The standard deviation of the clusters has implications about the smallest resolvable MU. This is discussed in Section 4.4.

4.3.5 TWITCH POTENTIATION

Figure 28 shows a second trial run of stimulations. In this figure the bands that indicate MU contributions increase and decrease with time and stimulation. This is due to twitch potentiation, which is explained in detail in Section 4.2.2.

Estimating the distance between the bands is difficult for potentiated data. A histogram of EPLA values for this data would be 'smeared' by the changing force production of the MUs. Breaking the data into subsets made calculating the EPLA for a specific MU simpler.

In people with myasthenia gravis the twitch potentiation is affected (Slomic, 1968), and a trial run such as shown in Figure 28 may be useful in quantifying the potentiation and determining if the subject has myasthenia gravis.

Figure 28
Trial Run 2

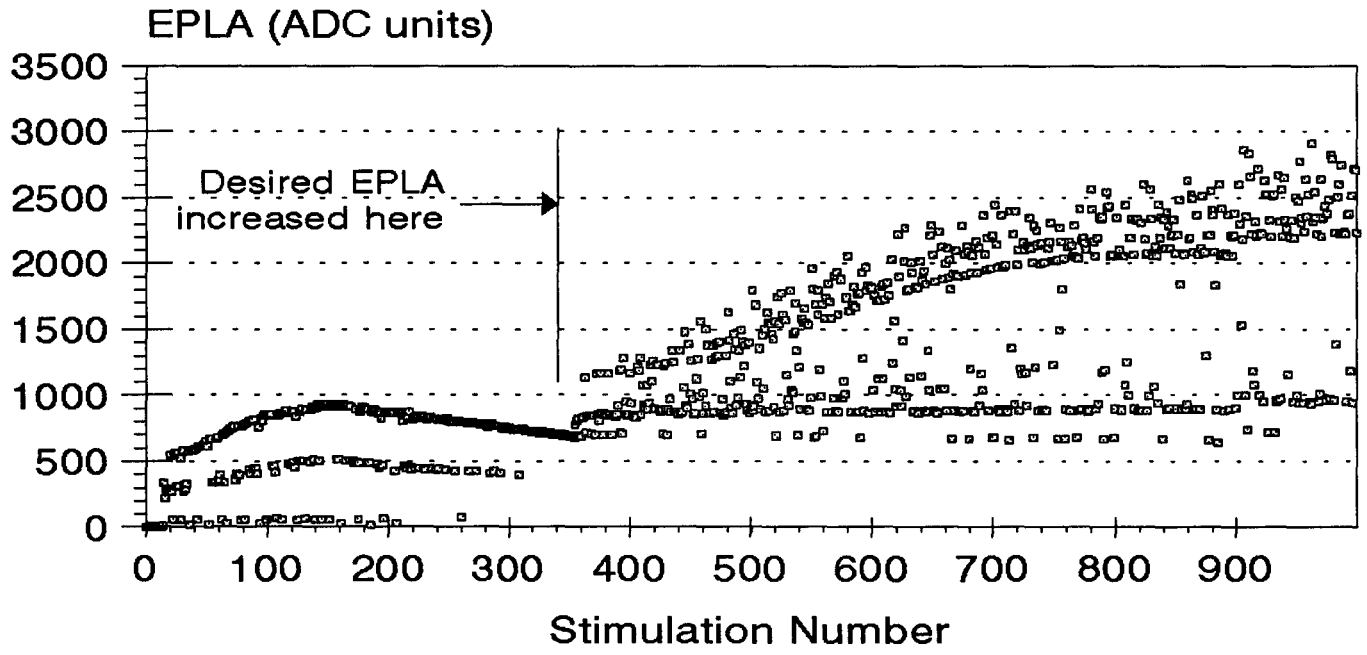

Constant acceleration mode
EPLA gain = 7521

Spike triggered averaging typically involves the averaging of 500 MU force responses. Figure 28 clearly shows that some, not all, MUs potentiate to several times the force output compared to their unpotentiated levels. This is not surprising since the MU may be fast or slow twitch. The averaging of many MU responses may result in an overestimation of MU size, and therefore an underestimation of MU numbers. Stein et al. (1990) found that force estimation techniques such as spike triggered averaging and intramuscular microstimulation tend to produce lower estimates than popular electrophysiological MU estimation procedures. These researchers attributed the lower estimates to excessive alternation in the electrophysiological procedures, although twitch potentiation would also account for the lower estimates from the MU estimation procedures based on force. It is important to note that the electrophysiological MU estimation procedures gave MU numbers closer to those found by anatomical data. (De Faria et al., 1978; Feinstein et al., 1955; Lee et al., 1975)

4.3.6 ACTIVATION CURVE CALCULATION

The firing probability curve for the MUs under investigation can be estimated. The program NN.C clusters points of the transfer function within a user specified radius

distance from each other. The transfer function is the graph of EPLA versus stimulus amplitude and is shown in Figure 26. Table 2 shows the results of a clustering analysis using a stimulus threshold of 44 mV and an acceleration threshold of 18 ADC units.

Deriving the activation curves for each of the MUs involves integrating and normalizing the EPLA clusters. This is done by choosing a stimulus voltage and calculating the percentage of points within the cluster that have been stimulated with lower stimulus amplitudes. Figure 29 shows some activation curves calculated in this way. The data points that were used for the activation curve estimation can be seen in Figure 25 and Figure 26.

4.3.7 FILTERING EFFECTIVENESS

To evaluate the effectiveness of the optimal filtering scheme explained in Section 3.3.3 and the momentum measure outputted by the TWITCH.C software, the degree of separation of the clusters can be calculated. If each data set is clustered with equivalent clustering thresholds, a higher number of clusters indicates better separation. If the clusters become less separable, then the filtering procedure is not useful. If the bands are more separable, the MU

Table 2

Clustering Results

Stimulus Threshold = 44mV, Acceleration Threshold = 18 Units

Figure 26 Reference	Number of Points	Stimulus Mean (Volts)	Acceleration Mean (ADC Value)
	1	47.29	887
Cluster #6	18	47.54	2554.56
	1	47.68	1863
	4	47.11	1137.75
Cluster #1	128	47.15	1017.72
	2	47.39	2639.5
	1	47.63	1836
Cluster #5	27	47.49	2221.7
Cluster #4	134	47.36	1987.93
	1	47.60	2367
	2	47.41	2391
Cluster #3	295	47.33	1647.49
Cluster #2	280	47.27	1336.33
	1	47.21	1171
	2	47.65	2132.5
	1	47.82	2452
	1	47.26	2318

For original data see Figure 26

Figure 29

Estimated Activation Curves

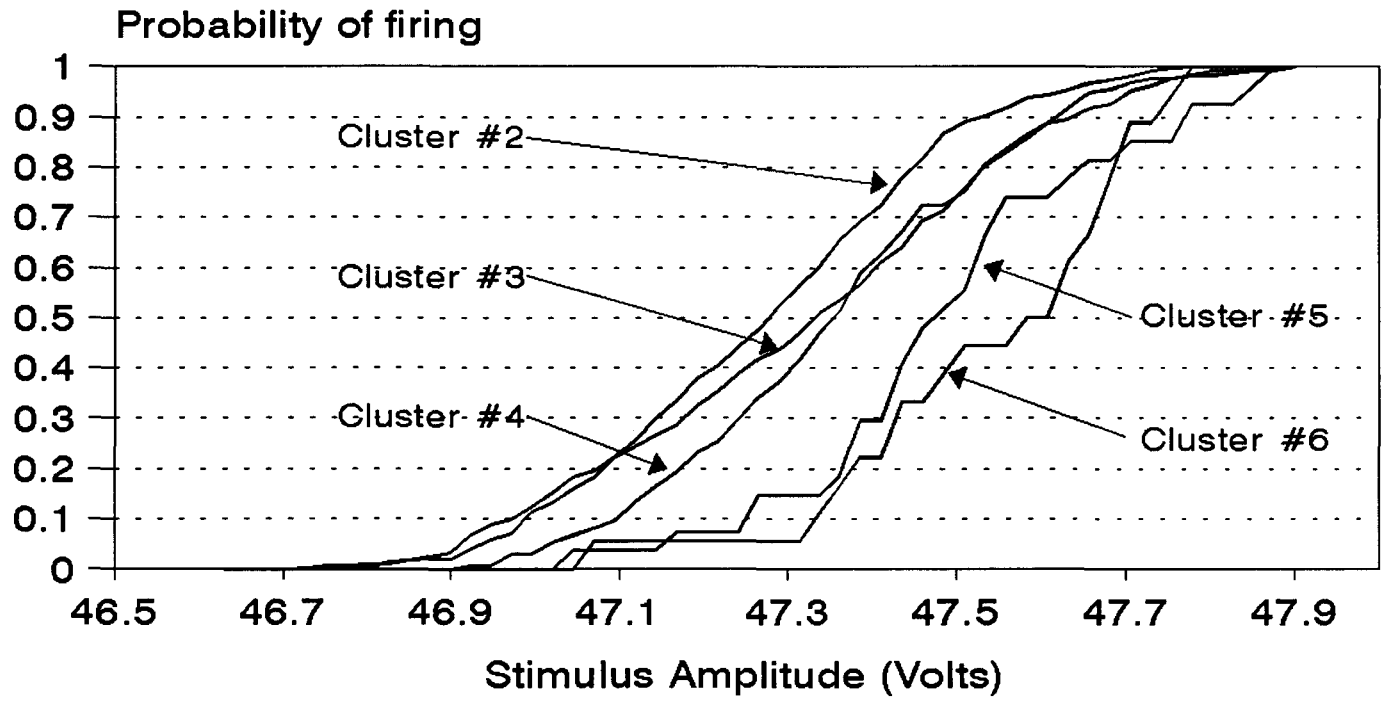

Derived from data in Figure 26

estimation procedures can be executed with greater accuracy and confidence.

The unfiltered data were clustered using the program NN.C using thresholds that separate all the visible bands. The clustering thresholds were then scaled to the filtered data and the momentum data. Scaling was necessary because the optimal filtering algorithm and the momentum calculation outputs a number proportional to pulse amplitude or pulse momentum respectively. The filtering procedure that produced the greatest number of clusters would be the best filtering procedure. Table 3 contains clustering data for various filtering procedures and scaling information. The data used for the clustering in this table came from Figure 26.

Table 3 shows that the clusters of the momentum data contained more points than the corresponding clusters of the optimally filtered or the unfiltered data. The clusters are more widely separated in the optimally filtered and unfiltered data than in the momentum data. Optimal filtering of muscle twitches does not help increase EPLA resolution over simply choosing the maximum point in the twitch. For simplicity, the unfiltered data will be used for MU estimation procedures in this thesis.

Table 3
Evaluating Filter Effectiveness
Using data shown in Figure 25

	Maximum Value	Minimum Value	Range	Acceleration Threshold	Number of Clusters
Peak Value Only	2648	887	1761	18	17
Optimally Filtered	122640	41340	81296	831	17
Momentum	157610	55350	104090	1064	13

All clustering procedures had stimulus threshold = 44 mV
Acceleration threshold chosen as constant ratio of range

4.3.8 MOTOR UNIT ESTIMATION BY CLUSTERING

This section deals with using the clustering program NN.C to calculate MU EPLA contributions. NN.C was used on the unfiltered responses previously numbered 100 to 1000 for the activation curve calculation in Section 4.3.6 and the significant clusters of the same data will be used again. Table 4 contains some basic clustering calculations.

The clustering method used for generating Table 4 is explained in detail in Section 3.4.3. Clustering thresholds were set to 18 ADC units for acceleration and 44 mV for stimulus amplitude. Cluster 1 corresponds to a EPLA baseline and the acceleration difference between cluster #1 and cluster #2 indicates a MU EPLA contribution.

Table 4 shows how MU EPLA contributions are calculated and how estimates of average MU EPLA contribution are made. As discussed in Section 4.1, the individual MU EPLA contribution calculations may be skewed toward the average. However, this does not affect the validity of the average MU EPLA contribution calculation.

The size of the MUs shown in Table 4 are approximately 300 ADC units at an amplifier gain setting of 28573 and an A/D range of 12 bits over +/-10 volts. Since the accelerometer

Table 4
MU EPLA Contribution Calculation

	Stimulus Mean (Volts)	Acceleration Mean (ADC Value)
Cluster #1	47.15	1017.72
Cluster #2	47.27	1336.33
Cluster #3	47.33	1647.49
Cluster #4	47.36	1987.93
Cluster #5	47.49	2221.7
Cluster #6	47.54	2554.56
	Between Clusters	MU MPLA
MU #1	1 and 2	318.6
MU #2	2 and 3	311.1
MU #3	3 and 4	340.4
MU #4	4 and 5	233.8
MU #5	5 and 6	332.9
Average MU MPLA	307.4	Gain setting
	ADC Units	28573

For original data see Figure 26
Acceleration gain setting = 28573

has a sensitivity of 9.6 mV/G, the approximate acceleration contribution of a single MU is about,

$$\sim 300\ ADC \times \frac{20V}{4096\ ADC} \times \frac{1\ V}{28573\ V} \times \frac{1\ g}{9.6e\text{-}3V} \times \frac{9.8 m/s^2}{1\ g} =$$

$$5.23\text{e-}5\ m/s^2 \text{ for typical MU EPLA}$$

4.3.9 MOTOR UNIT ESTIMATION BY AUTOCORRELATION

Another way to estimate the average MU EPLA contribution in data such as shown in Figure 25 is to look for fluctuations in the density of the points with respect to EPLA. This is similar to the very common problem of finding the centre frequency of a signal buried in noise. A method to estimate the average MU EPLA contribution is as follows:

1) Approximate acceleration density with a histogram with many bins
2) Do autocorrelation on acceleration density
3) Peak in autocorrelation determines average MU EPLA contribution

The density function of data from Figure 25 was estimated using a histogram with 1000 bins, and this is shown in Figure 30. Figure 31 shows the autocorrelation function of the

histogram for positive lags. Peaks in the autocorrelation function will correspond to the average MU EPLA contribution and there will also be peaks at integer multiples of that size. The first peak in the autocorrelation function for this data set occurs at 180 lags.

The histogram ranges from 888 ADC units to 2647 ADC units of EPLA and splits this range into 1000 bins. Therefore, the average MU EPLA contribution is (2647-888)/1000*180 = 316 ADC units. This agrees well with the MU EPLA contribution estimation using the NN.C program and is slightly easier to use.

This MU estimation algorithm works best for MUs with nearly similar sizes. Widely varying MU EPLA contributions will blur the peaks in the autocorrelation of the density estimation. If this happens, choosing the specific peak that indicates the average MU EPLA contribution may be difficult. In this case, the clustering program NN.C should be used to evaluate individual cluster sizes and an average MU EPLA contribution can then be determined.

Figure 30
Density Estimation

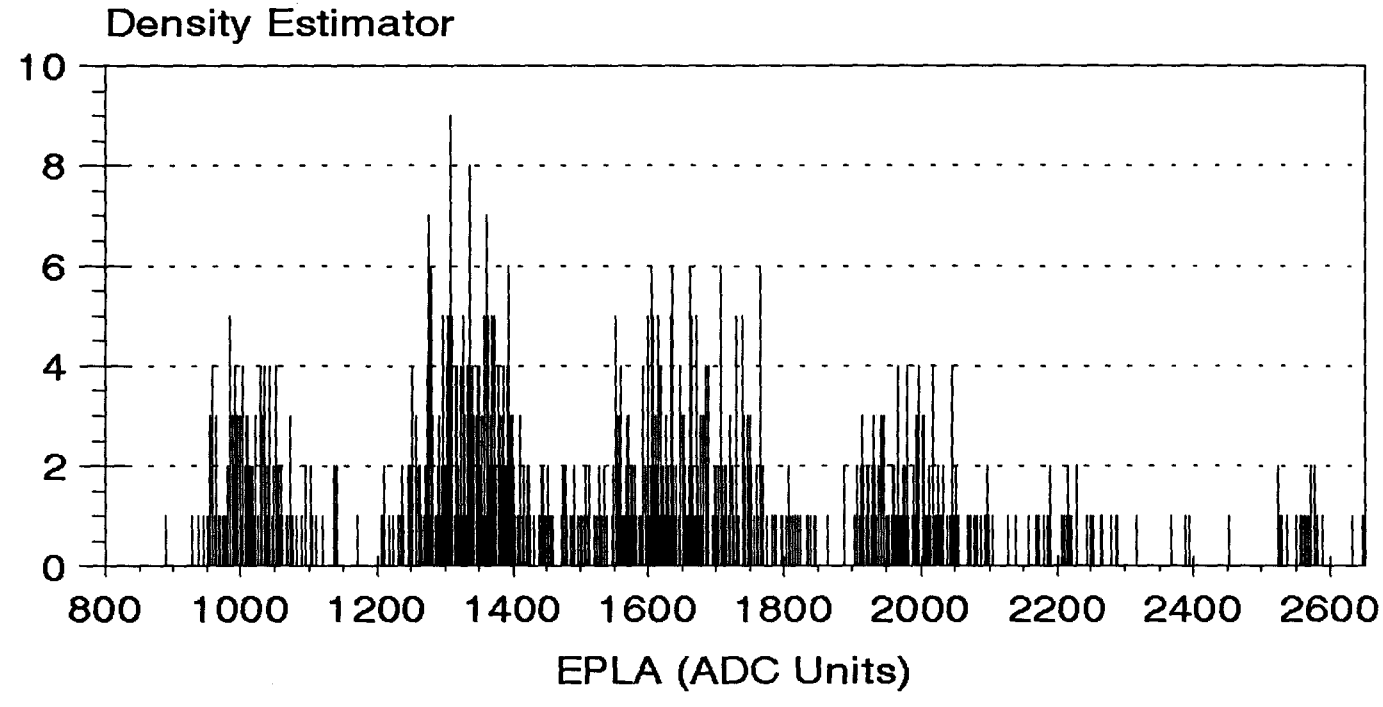

Contains points 100 to 1000 from Figure 25

Figure 31

Autocorrelation of Density
Positive Lags Only

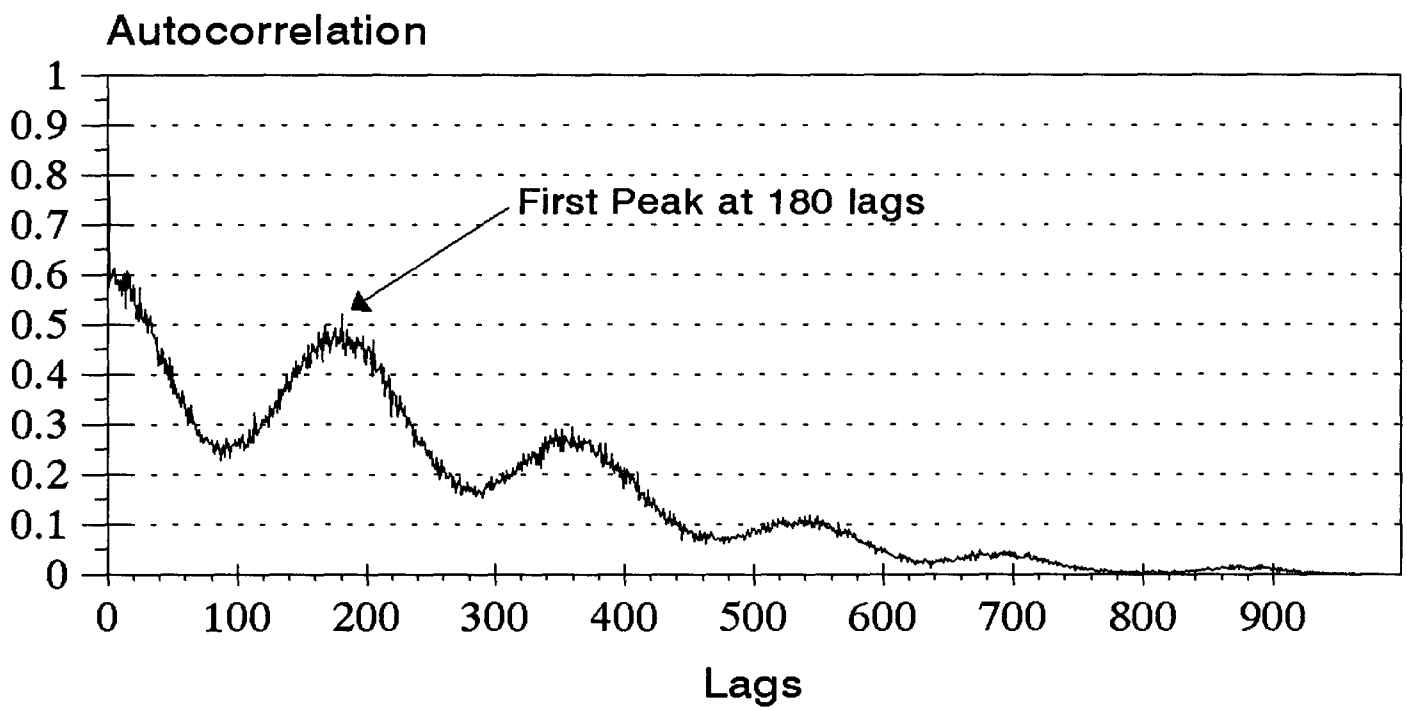

Density Estimation shown in Figure 30

4.4 SMALLEST RESOLVABLE MOTOR UNIT

The MU investigation techniques in this thesis rely on the separation of responses with different means in the presence of noise. The noise is shown to be approximately Gaussian in Section 4.3.4 and the resolution of a particular MU is dependent on MU EPLA contribution and noise amplitude. If MU EPLA contribution are small, the clusters in the transfer function for those MUs will have similar means and the amount of noise present will determine if the clusters are separable or not. For a given amount of noise there is a lower limit to the discernable MU size.

The amount of noise is primarily determined by mechanical noise sources and subject involuntary muscular control (see Section 2.3.4 and Section 2.3.6) and therefore the amount of noise present in a data set cannot be known before the experiment.

Because of the manner in which the EPLAs are gathered, there may not be a uniform number of points in each cluster. If a cluster contains only a few points, then that cluster must be sufficiently far away from other clusters for an MU EPLA contribution to be identified. Denser clusters may have a few hundred points in them. If two clusters have 100 points each then the smallest resolvable MU EPLA contribution for

visible separation of the clusters is about 3 to 4 times the standard deviation of the noise present. Figure 27 shows cluster 2 from Figure 26. Since the standard deviation of the noise for cluster #2 is 53.4, the smallest resolvable MU EPLA contribution for that trail run is 53.4*(3 to 4) = 160 to 213. Section 4.7 examines the effects of smallest resolvable MU EPLA contribution calculations on MU number estimations.

4.5 FINDING MAXIMUM EVOKED LIMB ACCELERATION

The MELA of the FDI occurs when all MUs are stimulated simultaneously. This requires a large stimulus and any further increases of stimulus intensity would not produce greater magnitude response.

The MELA of the index finger was found by using the ramp mode of the TWITCH.C software. In this mode, the stimulus intensity is varied to produce a ramp in EPLA. When all the MUs in the FDI are being stimulated, further increases in stimulus intensity do not produce increased limb acceleration. In subsequent stimulations, stimulus intensity would rise quickly and the EPLA would not progress higher than its maximum. A typical response using the ramp mode that shows the maximum response of the FDI is shown in Figure 32.

Figure 32
Finding MELA

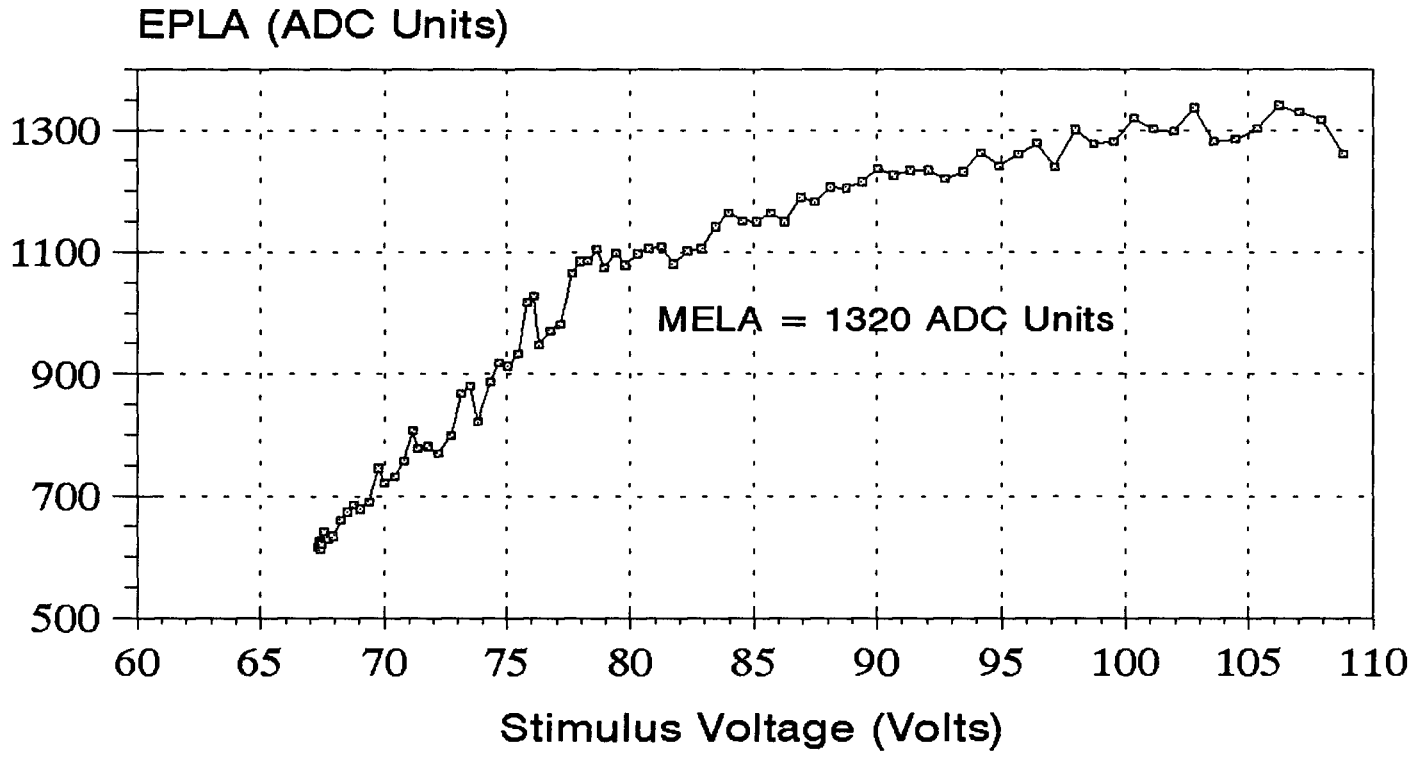

EPLA gain = 235

The EPLA clearly levels off to slightly above 1300 ADC units. The average response for stimulus amplitudes higher than 100 volts is 1320 ADC units. This is how the MELA was calculated. The amplifier gain setting for this run was 235.

The stimulation rate was approximately 4 Hz. The exact stimulus rate is not known since the computer stimulates as fast as possible while avoiding twitch fusion and excessive background noise. Since all of the MUs are stimulated during a maximum response, each of them may exhibit twitch potentiation by changing their force contribution.

4.6 DATA REPRODUCIBILITY

Studies of nerve excitation (Erlanger and Gasser, 1937) suggest that MU recruitment order for evoked stimulation is determined by the threshold of the MU axon and that MU threshold is inversely proportional to MU size. This implies that large MUs are recruited earlier than small MUs for increasing stimulus. Throughout the course of this thesis, no evidence of this correlation was found. However, it must be noted that only a few subjects were tested. It was found that MU recruitment order is very sensitive to electrode placement. Studies using graded nerve stimulation at the wrist for thenar EMG studies (Galea et al., 1991) have come to similar

conclusions while using many more subjects.

The physical distribution of the MU axons within the end plate zone is probably responsible for the variation of recruitment order with electrode position. Although large motor axons may have lower electrical thresholds, the current density produced by the stimulating electrodes at the axon is a stronger determinant of recruitment order. MU axons in a region of higher current density are generally recruited earlier than MU axons farther from current flow.

4.7 MOTOR UNIT NUMBER ESTIMATION EXAMPLE

Since the bands in Figure 25 are related to MU EPLA contribution and MELA responses can be determined, estimates of the number of MUs in a muscle can be made. If MELA is divided by the average MU EPLA, the result is the number of MUs in that muscle. MU counting is very valuable for the study of neuromuscular disorders.

For example, the following tests were successively performed on a subject who has no known neuromuscular disorders:

1) Subject's end plate zone determined (see Section 2.4.2)
2) Ramp to maximum - Figure 33 (see Section 4.5)
3) Ramped force mode - Figure 34 (see Section 3.3.4)
4) Electrode moved 3 mm towards fingertip
5) Ramp to maximum - Figure 35
6) Ramped force mode - Figure 36
7) Electrode moved 3 mm towards wrist
8) Ramp to maximum - Figure 37
9) Ramped force mode - Figure 38
10) Electrode moved 3mm towards thumb
11) Ramp to maximum - Figure 39
12) Ramped force mode - Figure 40

Smallest resolvable MU calculations were done for these tests. Data points in the band that separates MU #1 and MU #2 in Figure 34 were processed as described in Section 4.4. The smallest resolvable MU EPLA contribution is approximately 148 ADC units. This corresponds to 1/850 of the MELA. This lower limit to resolvable MU EPLA contribution does not significantly affect the MU estimates presented for this subject. If the smallest resolvable MU for a particular subject is near the same size of the average MU size, then MU EPLA contributions that are smaller than average will be indistinguishable from noise, and the average MU EPLA contribution will be artificially high.

Figure 33
MELA Estimation 1

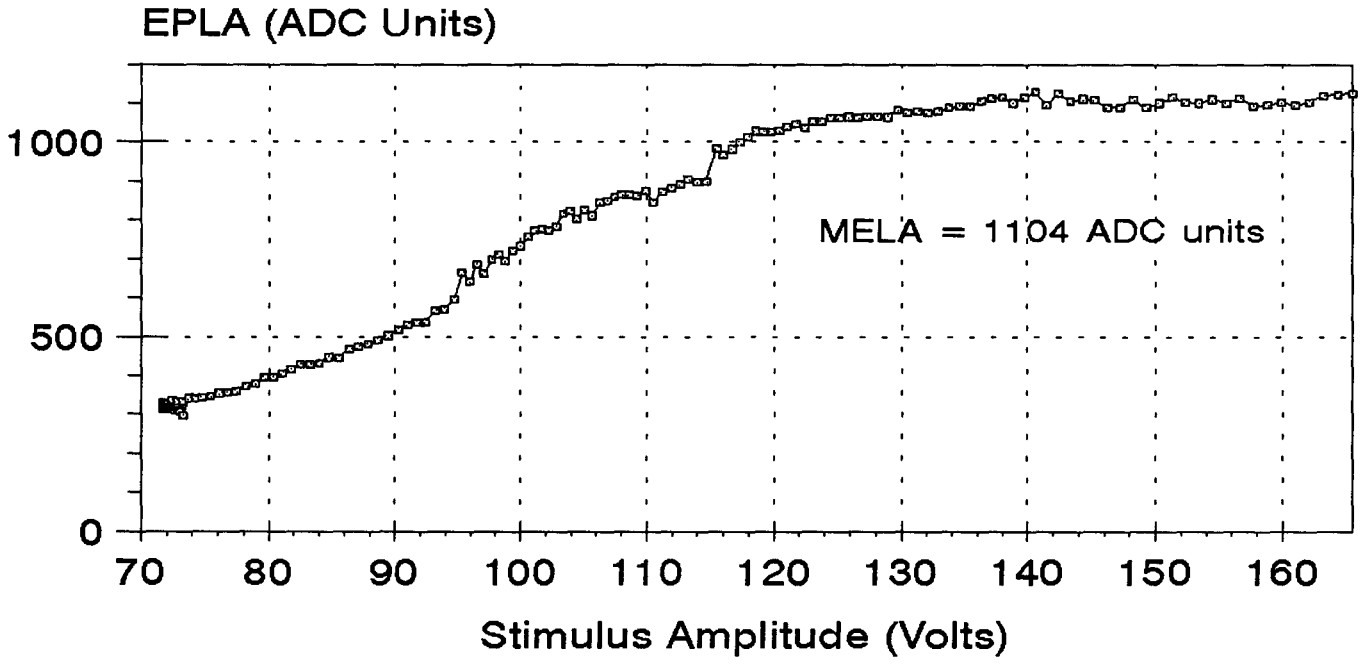

Ramp in force mode
EPLA gain = 235

Figure 34
MU Estimation 1

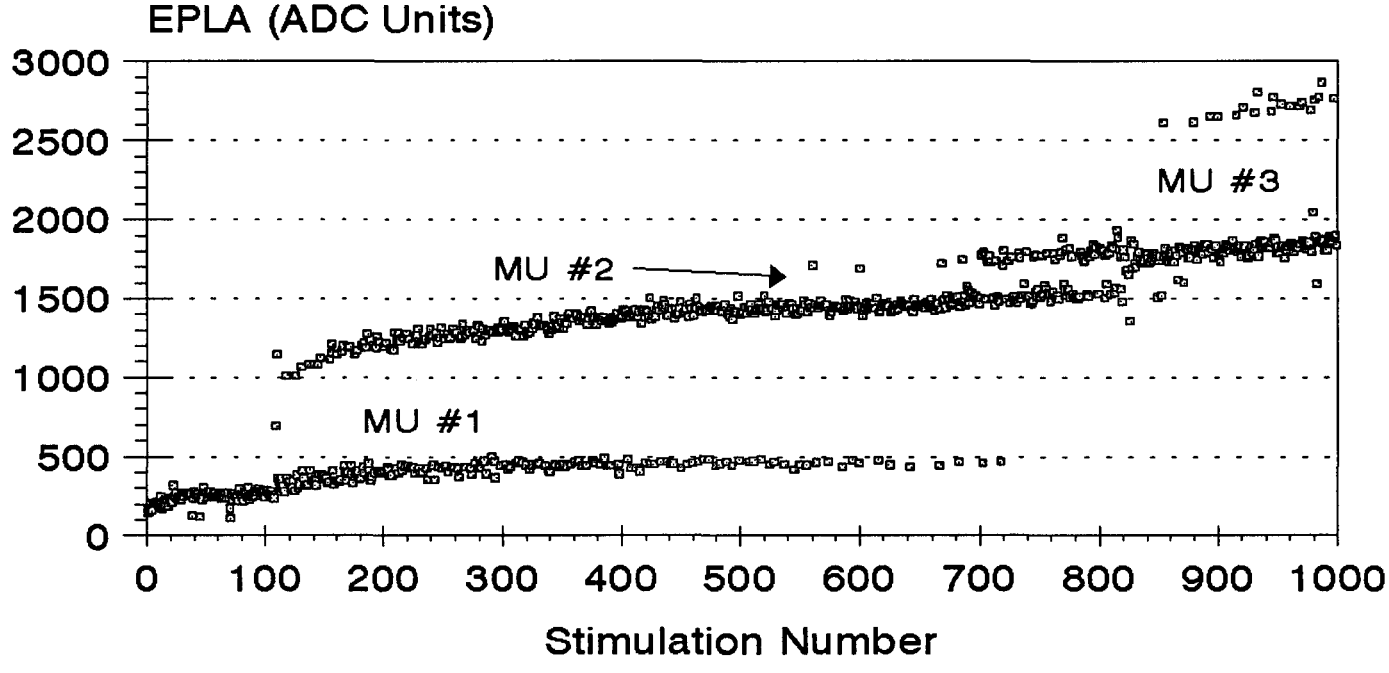

Ramp in force mode
EPLA gain = 28573

Figure 35
MELA Estimation 2

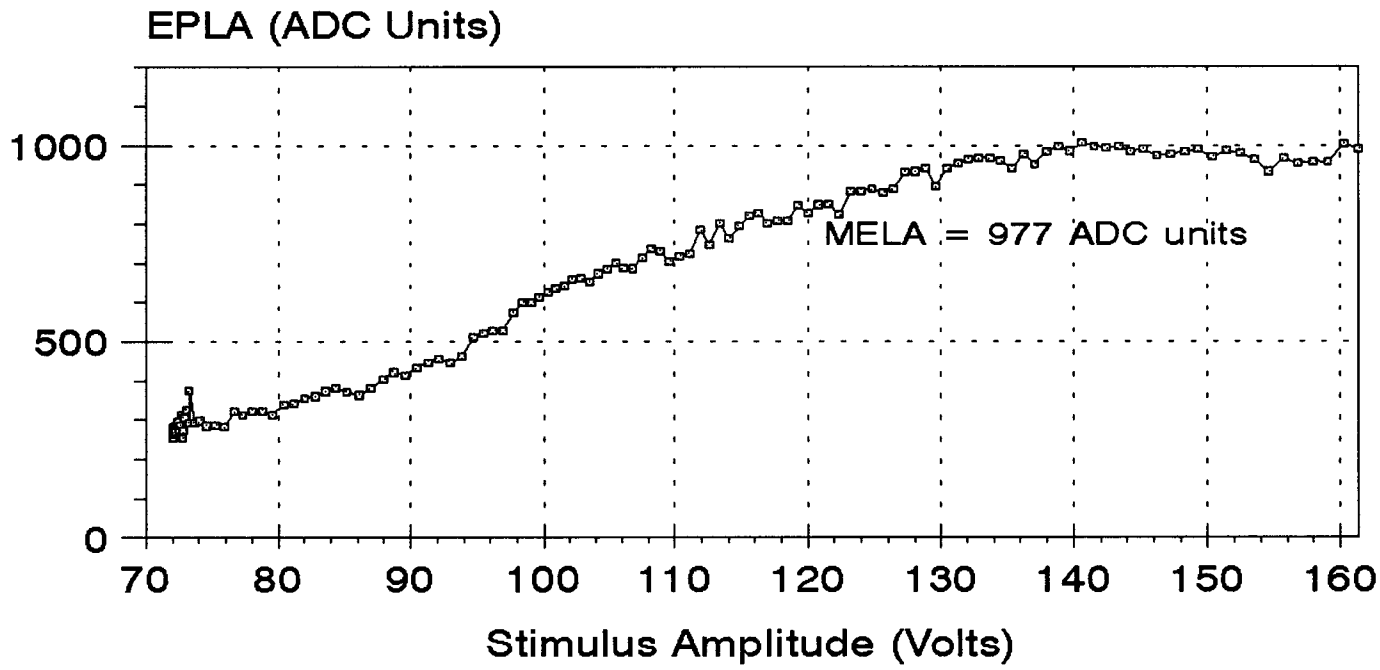

Ramp in force mode
EPLA gain = 235

Figure 36
MU Estimation 2

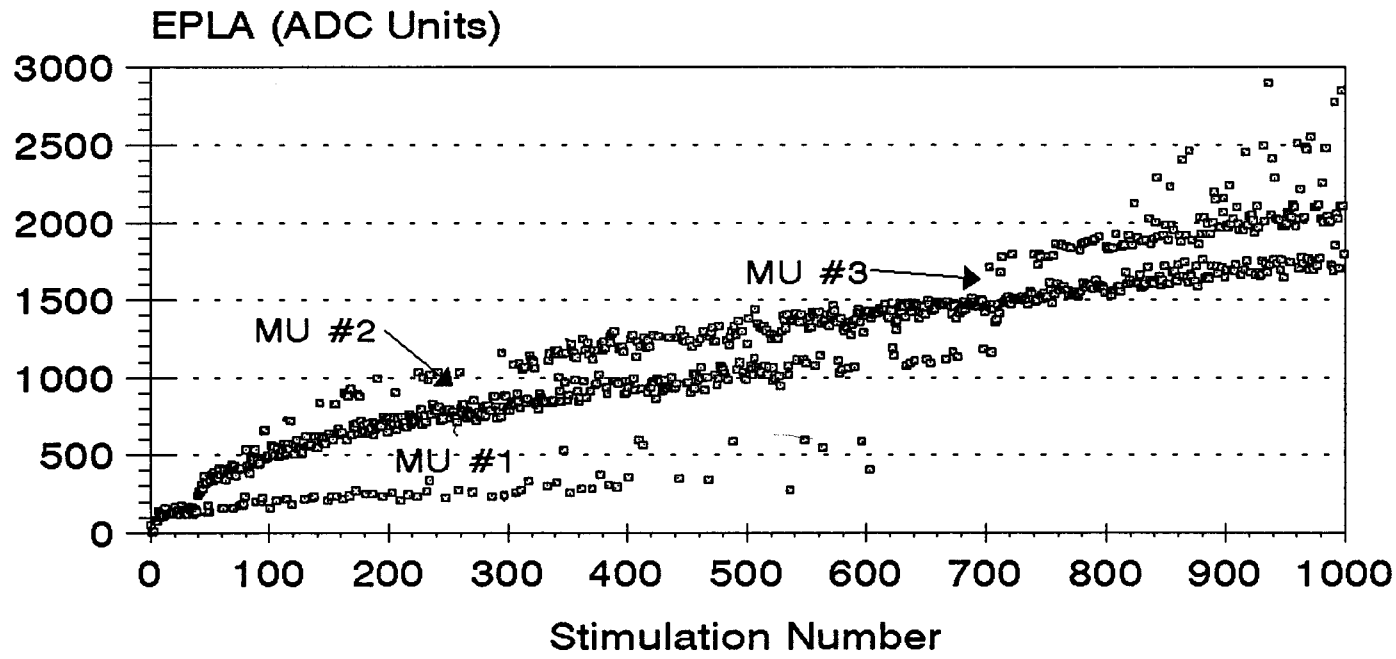

Ramp in force mode
EPLA gain = 28573

Figure 37
MELA Estimation 3

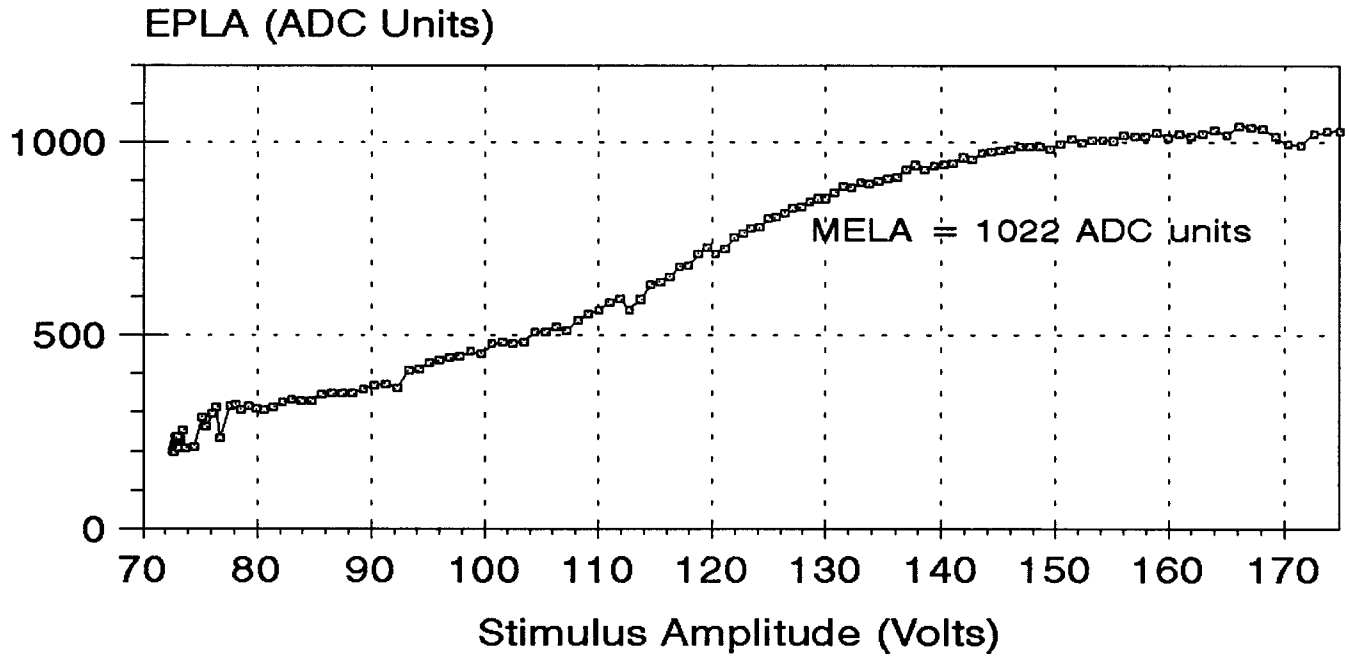

Ramp in force mode
EPLA gain = 235

Figure 38
MU Estimation 3

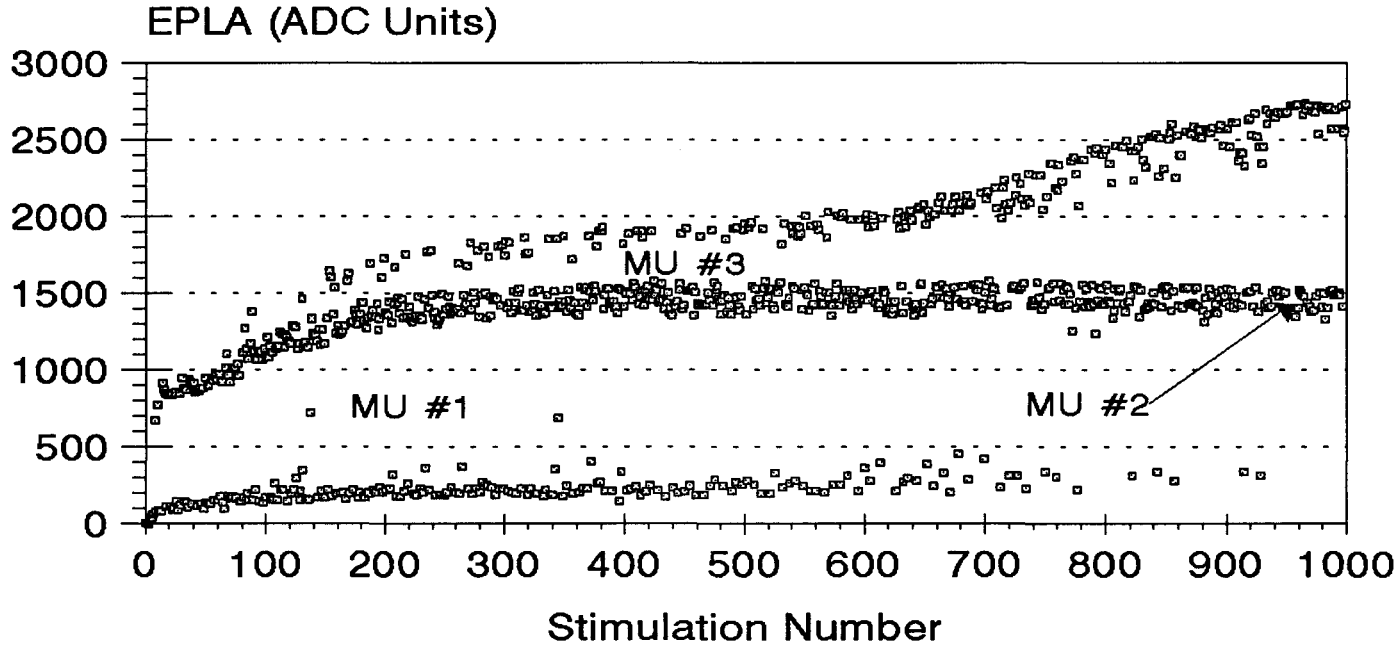

Ramp in force mode
EPLA gain = 7521

Figure 39
MELA Estimation 4

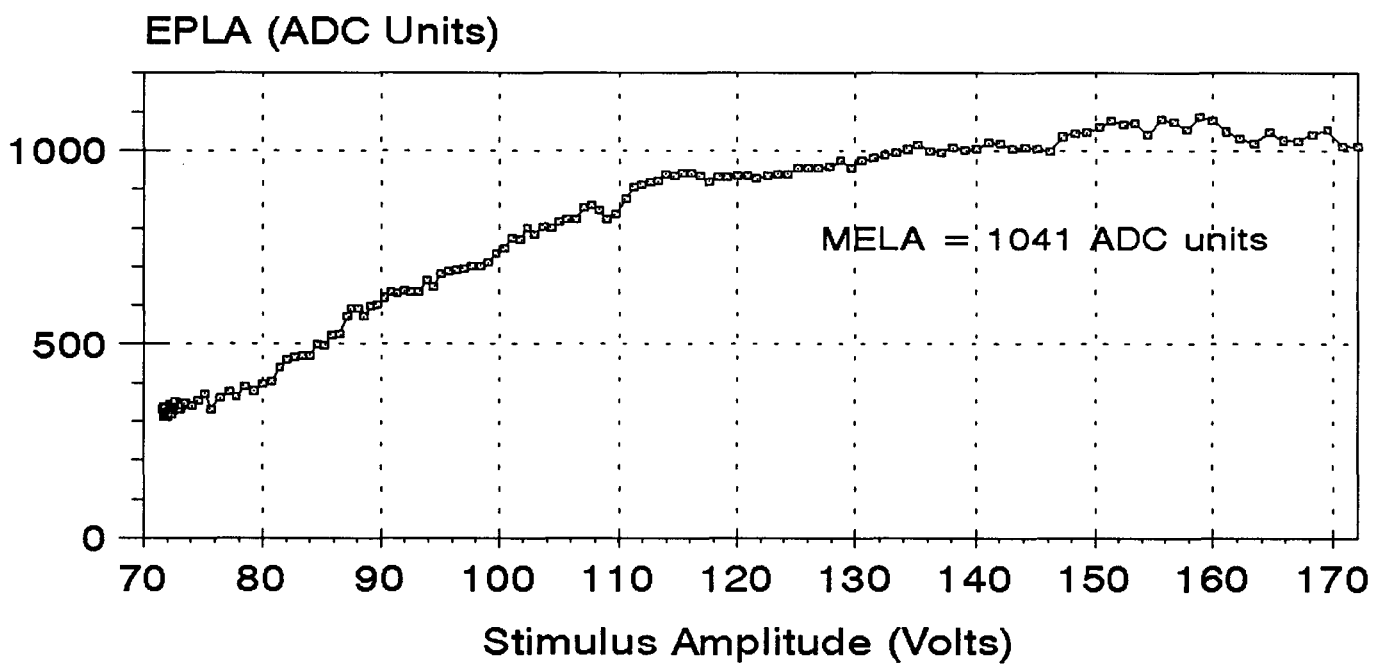

Ramp in force mode
EPLA gain = 235

Figure 40
MU Estimation 4

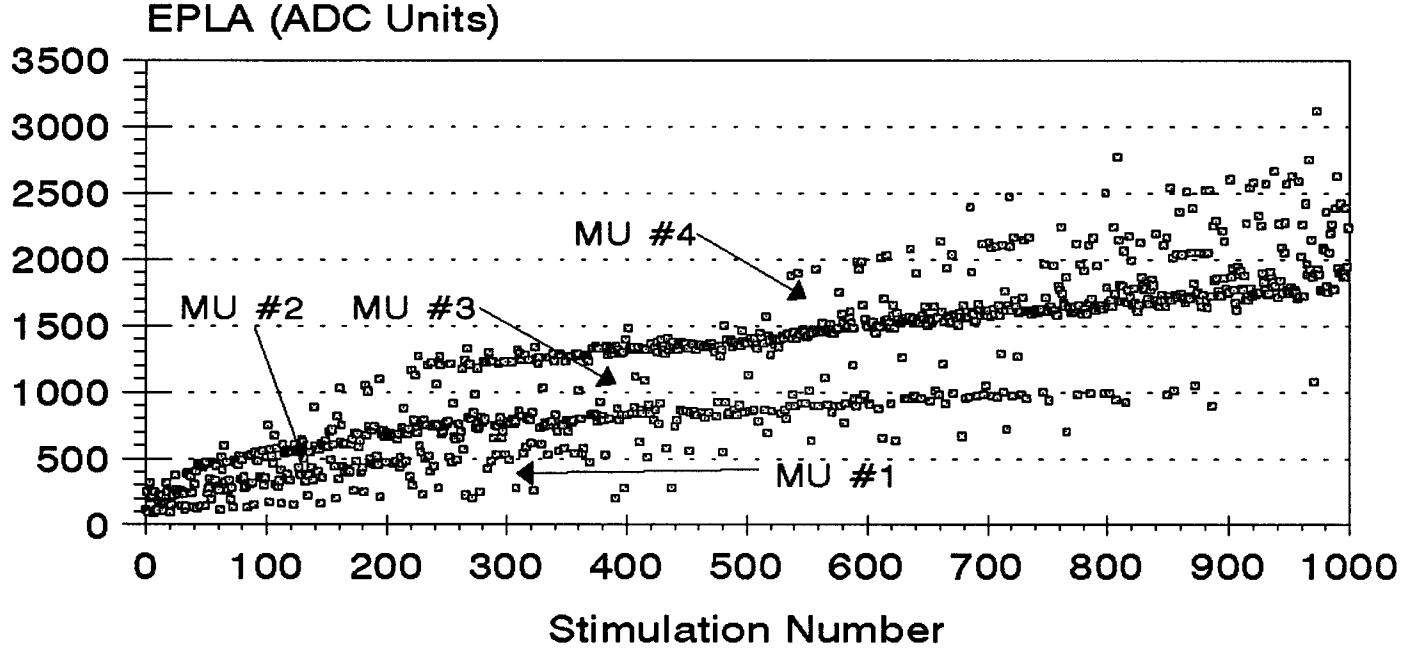

Ramp in force mode
EPLA gain = 25873

The MU sizes for each run were calculated using the software NN.C described in Section 3.4.1. Every effort was made to calculate the MU EPLA contributions under the same potentiated conditions as in the MELA test. This is why each MU estimation trial run immediately follows a MELA estimation run.

In the ramped force mode of the TWITCH.C software, some MUs are not stimulated until late in the test. Those MUs have a period of inactivity between the MELA estimation run and their stimulation in the MU EPLA contribution run. This inactive period may affect that MUs potentiation. For example, a MU may potentiate during the MELA estimation run if the MUs effective firing frequency is within the range for potentiation for that MU, then de-potentiate during its inactive period and then again potentiate during the MU EPLA estimation run. However, the degree to which this occurs was considered too difficult to calculate for every MU estimated. Therefore, the stimulation rate is made as high as possible while avoiding twitch fusion in the estimation of the MELA and only the initially observable MU EPLA contributions are used for MU number estimations.

The estimate of the number of MUs in the FDI for this subject is shown in Table 5. The gains of each trail run were

Table 5

MU Estimation Calculations

Data from :	MU EPLA Contribution	ADC Gain	Related MELA
Figure 34	MU #1 = 850 MU #2 = 1009 MU #3 = 894	28573	Figure 33 = 1104
Figure 36	MU #1 = 230 MU #2 = 233 MU #3 = 284	28573	Figure 35 = 977
Figure 38	MU #1 = 772 MU #2 = 97 MU #3 = 327	7520	Figure 37 = 1022
Figure 40	MU #1 = 181 MU #2 = 206 MU #3 = 327 MU #4 = 486	28573	Figure 39 = 1041
Average MU EPLA	840	Normalized	
Average MELA	125960	Normalized	
MU Number Estimation	150	Motor Units	

Gain setting for all MELA calculations is 235

taken into account before average MU EPLA calculations or MU number estimates were made. This subject has approximately 150 MUs in his FDI. This is within a reasonable range for FDI motor units.

Figure 38 shows an interesting effect of twitch potentiation. Before stimulation number 100, MU #3 was not stimulated. Between stimulation numbers 100 and 600, it has a relatively low effective firing frequency. As MU #1 begins to fire more frequently, MU #3 fires more frequently and its effective firing frequency enters the range in which twitch potentiation occurs for that particular MU. MU #3 then potentiates to a new EPLA contribution. It is not known whether MU #3 stops potentiating due to its effective firing frequency leaving the range in which potentiation occurs, or due to physiological limits.

In Figures 34, 36, 38, and 39 we can see the MU EPLA contribution change over time due to twitch potentiation. Some MU EPLA contributions potentiate to over three times their unpotentiated EPLA contributions. If twitch potentiation is ignored in a MU estimation procedure, MU estimates may vary extremely widely. Therefore, one cannot ignore twitch potentiation when estimating MU properties

through their force contributions if those MUs are stimulated several times.

Average MU counts using this technique for the general population were not performed.

CHAPTER 5.

CONCLUSIONS

The use of accelerometers to measure EPLA allows a unique view of the force properties of MUs. It is non-invasive and clearly shows that twitch potentiation must be taken into account in MU estimates in which the MU is stimulated more than several times. MU number estimates can be made from EPLA data from human skeletal muscle. Stein et al. (1990) found that MU number estimates based on force using intramuscular microstimulation and spike-triggered averaging were substantially lower than electrophysiological estimates using graded whole nerve stimulation at the wrist. These researchers attributed the difference in MU number estimates to greater alternation in the studies using graded whole nerve stimulation. However, this thesis shows that twitch potentiation may also account for lower MU number estimates based on force in which MUs are repeatedly stimulated.

Veltink et al. (1990) showed that discrete levels in the muscle force versus stimulus amplitude relationship represent individual MU contributions. Their study involved rats and required the severing of the extensor digitorum longus and tibialis anterior tendons for force measurements and the use

of intrafasicular electrodes for stimulation. They were unable to demonstrate these discrete levels using extraneural electrodes. The present study shows that discrete levels in the muscle force versus stimulus amplitude relationship can be achieved non-invasively for human FDI muscles with the use of accelerometers and the measurement of EPLA.

The techniques described in this thesis are useful for the investigation of many MU properties including recruitment order, twitch potentiation, alternation and MU size. MU number estimates can be made based solely on acceleration information. In addition, the activation curves for several MUs may be estimated. Calculations of the smallest resolvable MU can be made and the validity of a MU estimate can be quantitatively evaluated.

Blood pressure and respiration did not significantly affect the MU measurements as they did in muscle force studies using strain gauges by Westling et al. (1990). This is probably due to the high pass filtering in the accelerometer amplifier and the inherent baseline fluctuations reductions when measuring limb acceleration. Studies using strain gauges may benefit from high pass filtering.

It is very important to note that the techniques used for alternation detection and MU estimation developed in this thesis can also be applied to data from strain gauge force measurement systems, which may allow alternate MU estimates.

CHAPTER 6.

FUTURE WORK

MU force contributions change over time during repetitive stimulation. The techniques in this thesis required relatively constant MU force contributions and therefore only data subsets could be used for determining MU EPLA contributions. If techniques were created that could determine MU EPLA contributions from data sets that contain potentiating MUs, then more MU information could be gathered. Early results using three dimensional clustering on EPLA, stimulus amplitude and time of stimulation look promising. However, it does not solve the problem of quantifying the state of potentiation of MU EPLA contribution and in the MELA calculation for accurate MU number estimation. Perhaps large stimuli for determination of the MELA could be randomly interspersed between the smaller stimuli used for determining the individual MU EPLA contribution . This would ensure that MU EPLA contribution is in the same state of potentiation as in the MELA. The gain of the accelerometer would then have to be digitally controlled by the computer, and the controlling software modified.

The clustering analysis described in Section 3.4.3 requires an operator to use his or her judgement to determine clustering thresholds. Automating this step would allow MU estimates to be based solely on definable criteria, thus eliminating the need for operator judgement and reducing human error.

With a given set of MUs, there are many possibilities for alternated responses. However, some of those possibilities are very unlikely. A reduced set of non-alternated and probable alternated responses may be calculated and a non-linear least squares fitting of MU force response sizes to this reduced set may be extremely useful in automating MU estimations of this type.

APPENDICES

A.1: ACCELEROMETER SPECIFICATIONS

Model:	Entran EGAX-5
S/N:	91J91I20-P02
Range:	+/-5g
Bandwidth:	3 dB down at 540 Hz
Limit:	+/-10000g (in sensitive axis only)
Temperature Range, Compensated:	70°F to 170°F
Temperature Range, Operating:	-40°F to 250°F
Non-Linearity:	+/-1%
Output:	9.60 mv/g at 75°F and 50 Hz
Input Impedance:	811 ohms
Output Impedance:	458 ohms
Input Voltage:	15 Volts DC
Thermal Zero Shift:	+/-2.5%FS/100°F
Thermal Span Shift:	+1/-4%/100°F
Manufacture Site:	Fairfield, N.J., USA
Max Input Voltage:	18 Volts DC

A.2: ACCELERATION AMPLIFIER DESIGN PROCESS

The choice of components for this amplifier design is very important for adequate performance. Noise performance depends on matching driving impedances to opamps with suitable voltage and current noise characteristics. Improper choice of amps could cause the amplifier to have significant noise (Horowitz and Hill, 1989).

U2 should have input voltage noise and input current noise optimized for the impedance at the junction of the 20k and 2200uF first order filter. The opamp should also have a high open loop voltage gain and a low input offset voltage. The opamp must also be able to supply enough current for the accelerometer excitation voltage to be maintained. Almost any opamp can satisfy the open loop gain, input offset, and output current requirements, but the voltage and current noise need closer consideration. Over the frequency range required, an opamp that would be suitable would be an OP27EN8.

U1 should have a high input impedance, a very low input offset current, high voltage gain and a reasonably low input offset voltage. Since the amplifier is set up as a very slow

integrator, bandwidth is not of any consideration. Input noise voltage and input noise current should be optimized for operation from impedances of 1 Megohm in parallel with 10uF over the desired frequency range. U1 operates below the low frequency cutoff determined by R2, C2. A good choice for U1 would be an LT1012ACN8.

U3 provides common mode rejection and a negative excitation voltage for the accelerometer. Therefore, it must have enough output current for the accelerometer excitation voltage to be maintained. Input offset voltage is not important in this amplifier because offset errors would be exhibited as a DC offset at the input of U4 and would then be removed by the action of U1. U3 should be optimized for low noise operation from the bridge impedance of the accelerometer. Since this is relatively low, input voltage noise is of more importance than input noise current. If we also consider the limited gain of the opamp, the common mode signal is reduced to the amplitude of the error of U3 in an inverting mode with a gain of 1. The opamps chosen should have a very high open loop gain so that the error would be low over the frequencies of interest. Essentially, the common mode gain is inversely proportional to the open loop gain of U3. A good choice for U3 would be a OP27EN8.

U4 provides the voltage gain for the amplifier and must amplify the output of the accelerometer. U4 should have a high voltage gain for good accuracy. Its input voltage and current noises should be optimized for operating from the output impedance of the accelerometer. The output impedance of the accelerometer is approximately 800 ohms, and therefore a good choice for U4 is OP27EN8.

U5 provides signal inversion and DC offset. The DC offset is included because the analog to digital board provides input from -10 volts to +10 volts. (See Section 2.5.2) Since we are primarily interested in the positive peak acceleration (see Section 1.7), the DC offset allows greater gain without clipping and therefore greater resolution of the acceleration peaks.

The power supply for the accelerometer amplifier was provided by an separate dual regulated power supply. (Anatek model 25-20)

A.3 MUSCLE SIMULATION PROGRAM

The program ALT.M was written to simulate the peak force output of human muscles during electrical stimulation. It must run within the development system MATLAB. The program is as follows:

```
%-------------------------------------------------------------
%
%                       Program for...
%
%          Simulation of human muscle stimulation
%
%                  Doug Eleveld - July 1992
%
%-------------------------------------------------------------
clear;
% Random variable and graphics screen setup
rand('normal');
clg
format compact;
axis([0 600 0 20]);
hold on;

% This contains the peak force production of the motor units
forces = 1*[ 1 1 1 1 1 1 1 1 1 1 1 1 1 1 1 1 1 1 1 1 ];
forces = forces + rand(forces)*0.0;
forces
pause

% This variable contains the thresholds of the motor units
thresh = [ 1 2 3 4 5 6 7 8 9 10 11 12 13 14 15 16 17 18 19
20];

% This variable determines the degree of alternation
threshstd = 3;

% This variable adds white gaussian noise to the force output
noisestd = 0;

% Initialize the output matrix
allforces = zeros(200,2);
```

```
% This variable determines the stimulation intensity
stim = 5;

% Here we will simulate 600 stimulations
for stimnumber=1:600,
   threshnow = thresh+threshstd*rand(thresh); % Find threshold
   fired = find(threshnow<stim);              % Which MU's ?
   totforce = sum(forces(fired))+noisestd*rand; % Total force
   [x,numfired] = size(fired);                % Number fired
   allforces(stimnumber,1) = totforce;       % Save for later
   allforces(stimnumber,2) = numfired;       % Save for later
   stimnumber = stimnumber+1;                 % Next stimu
   plot(stimnumber,totforce,'.w');            % Just look

% A line here could modify the stimulus intensity
stim = stim + 7/600;

end                                           % Another stim?

% Fix up variables sizes
stimnumber = stimnumber-1;
allforces = allforces(1:stimnumber,:);
levels = cumsum(forces);
hold off;
plot(allforces(:,1),'.w');
hold on;
plot(levels,'+g');
hold off;
```

REFERENCES

Ballantyne J.P., Hansen S., "A new method for the estimation of the number of motor units in a muscle.
1. Control subjects and patients with myasthenia gravis", Journal of Neurology, Neurosurgery and Psychiatry, 37, 1974, 907-915.

Basmajian J.V., Muscles Alive: Their function revealed through electromyography, 4th Ed. Baltimore: Williams and Wilkins Co., 1979.

Burke D., Skuse N.F., Lethlean A.K., "Isometric contraction of the abductor minimi muscle in man", Journal of Neurology, Neurosurgery and Psychiatry, 37, 1974, 825-834.

Cavasin R., An Automated Muscle Motor Unit Counting System, Master's Thesis. Hamilton: McMaster University, 1989.

Clark J.W. Jr, Neumann M.R., Olson W.H, Peura R.A., Primiano F.P. Jr, Siedband M.P., Webster J.G., Wheeler L.A., Medical Instrumentation Application and Design, 2nd Ed. Boston: Houghton Mifflin Co., 1992

Data Translation Inc., User Manual for DT2801 Series Single Board Analog and Digital I/O Systems for the IBM Personal Computer, Massachusetts, Data Translation Inc, 100 Locke Dr., Malboro MA, 01752-1192, 1983.

Daube J.R., "Statistical estimates of number of motor units in thenar and foot muscles in patients with amyotrophic lateral sclerosis or the residue of poliomyelitis, Muscle and Nerve, 12, 1988, 957-A.

De Faria C.R., Toyonaga K, "Motor unit estimations in a muscle supplied by the radial nerve", Journal of Neurology, Neurosurgery and Psychiatry, 41, 1978, 794-797.

Desmedt J.E., Hainaut K., "Kinetics of myofilament activation in potentiated contraction: Staircase phenomenon in human skeletal muscle", Nature, 217, 1968, 510-532.

Entran International, Accelerometer Instruction & Selection Manual, Entran Devices Inc, 10 Washington Ave., Fairfield N.J., 07006, 1987.

Erlanger J., Gasser H.S., Electrical Signs of Nervous Activity, Philadelphia, University of Pensylvania Press, 1937.

Feinstein B., Lindegard B., Nyman E., Wohlfart G., "Morphologic studies of motor units in normal human muscles", Acta Anatomica, 23, 1955, 127-142.

Galea V., de Bruin H., Cavasin R., McComas A.J., "The numbers and relative sizes of motor units estimated by computer", Muscle & Nerve, 14, 1991, 1123-1130.

Gravel D., Belanger A.Y., Richards C.L., "Study of human muscle contraction using electrically evoked twitch responses during passive shortening and lengthening movements", European Journal of Applied Physiology and Occupational Physiology, 56, 1987, 623-627.

Horowitz P., Hill W., The Art of Electronics, New York, Cambridge University Press, 1989.

Jasechko J.G., Automatic Estimation of the Number of Muscle Motor Units, Master's Thesis. Hamilton: McMaster University, 1987.

Kadrie H.A., Yates S.K., Milner-Brown H.S., and Brown W.F., "Multiple point electrical stimulation of ulnar and median nerves", Journal of Neurology, Neurosurgery and Psychiatry, 39, 1976, 973-985.

Lee R.G., Ashby P., White D.G., Aquayo A.J., "Analysis of motor conduction velocity in the human median nerve by computer simulation of compound muscle action potentials", Electroencephalography and clinical neurophysiology, 39, 1975, 225-237.

Linear Technology Data Book for 1990, 1990 Linear Databook, Linear Technology Corporation, 1630 McCarthy Bvld., Milpitas CA, 95035, 1990

McComas A.J., Fawcett P.R.W., Campell M.J., and Sica R.E.P., "Electrophysiological estimation of the number of motor units within a human muscle", Journal of Neurology, Neurosurgery and Psychiatry, 34, 1971, 121-131.

McComas A.J., "Invited review: Motor unit estimation: Methods, results, and present status", Muscle and Nerve, 14, 1991, 585-597.

Milner-Brown H.S., Brown W.F., "New methods of estimating the number of motor units in a muscle", Journal of Neurology, Neurosurgery and Psychiatry, 39, 1976, 258-265.

Panayiotopoulos C.P., Scarpalezos S., and Papapetropoulos T., "Electrophysiological estimation of motor units in Duchenne muscular dystrophy", Journal of Neurological Sciences, 23, 1974, 89-98.

Parry D.J., Mainwood G.W., Chan T., "The relationship between surface potentials and the number of active motor units", Journal of Neurological Sciences, 33, 1977, 283-296.

Slomic A., "The staircase phenomenon in normal and in myasthenic human muscle", Society proceedings of Electroencephalography and clinical neurophysiology, 25, 1968, 396.

Stein R.B., Yang J.F., "Methods for estimating the number of motor units in human muscles", Annals of Neurology, 28, 1990, 487-495.

Stephens J.A., Usherwood T.P., "The mechanical properties of human motor units with special reference to their fatigueability and recruitment threshold", Brain Research, 25, 1977, 91-97.

Tortora G.J., Anagnostakos N.P., Principles of Anatomy and Physiology, 6th Ed. New York: Harper & Row 1990.

Veltink P.H., van Alste J.A., Boom H.B.K., "Multielectrode intrafasicular and extraneural stimulation", Medical & Biological Engineering & Computing, 27, 1989, 19-24.

Westling G., Johansson R.S., Thomas C.K., Bigland-Ritchie B., "Measurement of contractile and electrical properties of single human thenar motor units in response to intraneural motor-axon stimulation, Journal of Neurophysiology, 64, 1990, 1331-1338.

Wilmshurst T.H., Signal Recovery from Noise in Electronic Instrumentation, Bristol: Adam Hilger Ltd 1985.